Multi-Resolution Imaging through a Novel Bayesian Compressive Sensing Approach

N. Anselmi, L. Poli, G. Oliveri, and A. Massa

Abstract

In this work, a multi-resolution strategy is proposed for improving the reconstruction capabilities of standard Bayesian compressive sensing (*BCS*) when dealing with the imaging of sparse targets. Towards this end, a customized relevance vector machine (*RVM*) solver is derived and implemented in order to exploit the progressively acquired information about the scatterer shape and location within the imaged domain.
Some numerical results are shown to validate the effectiveness of the proposed imaging technique.

1 Numerical Results

1.1 Rhombus, $D = 1.5\lambda$

Test Case Description

Direct solver:

- Side of the investigation domain: $L = 6.0\lambda$
- Cubic domain divided in $\sqrt{D} \times \sqrt{D}$ cells
- Number of cells for the direct solver: $D = 1600$ (discretization $= \lambda/10$)

Investigation domain:

- Cubic domain divided in $\sqrt{N} \times \sqrt{N}$ cells
- Number of cells for the inversion:
  - First Step IMSA: $N^{(1)} = 100$ (discretization $= \lambda/10$)
  - Following Steps IMSA: $N^{(i)}$ not fixed, defined according to the estimated RoI $\mathcal{D}^{(i)}$

Measurement domain:

- Total number of measurements: $M = 60$
- Measurement points placed on circles of radius $\rho = 4.5\lambda$

Sources:

- Plane waves
- Number of views: $V = 60$; $\theta_{inc}^{v} = 0° + (v-1) \times (360/V)$
- Amplitude: $A = 1.0$
- Frequency: $F = 300$ MHz ($\lambda = 1$)

Background:

- $\varepsilon_r = 1.0$
- $\sigma = 0$ [S/m]

Scatterer

- Rhombus, $D = 1.5\lambda$
- $\varepsilon_r \in \{1.01, 1.02, 1.04, 1.05, 1.06, 1.08, 1.10, 1.15, 1.20\}$
- $\sigma = 0$ [S/m]

1.1.1 Rhombus, $D = 1.5\lambda$, $\tau = 0.02$ - IMSA-BCS reconstructed profiles

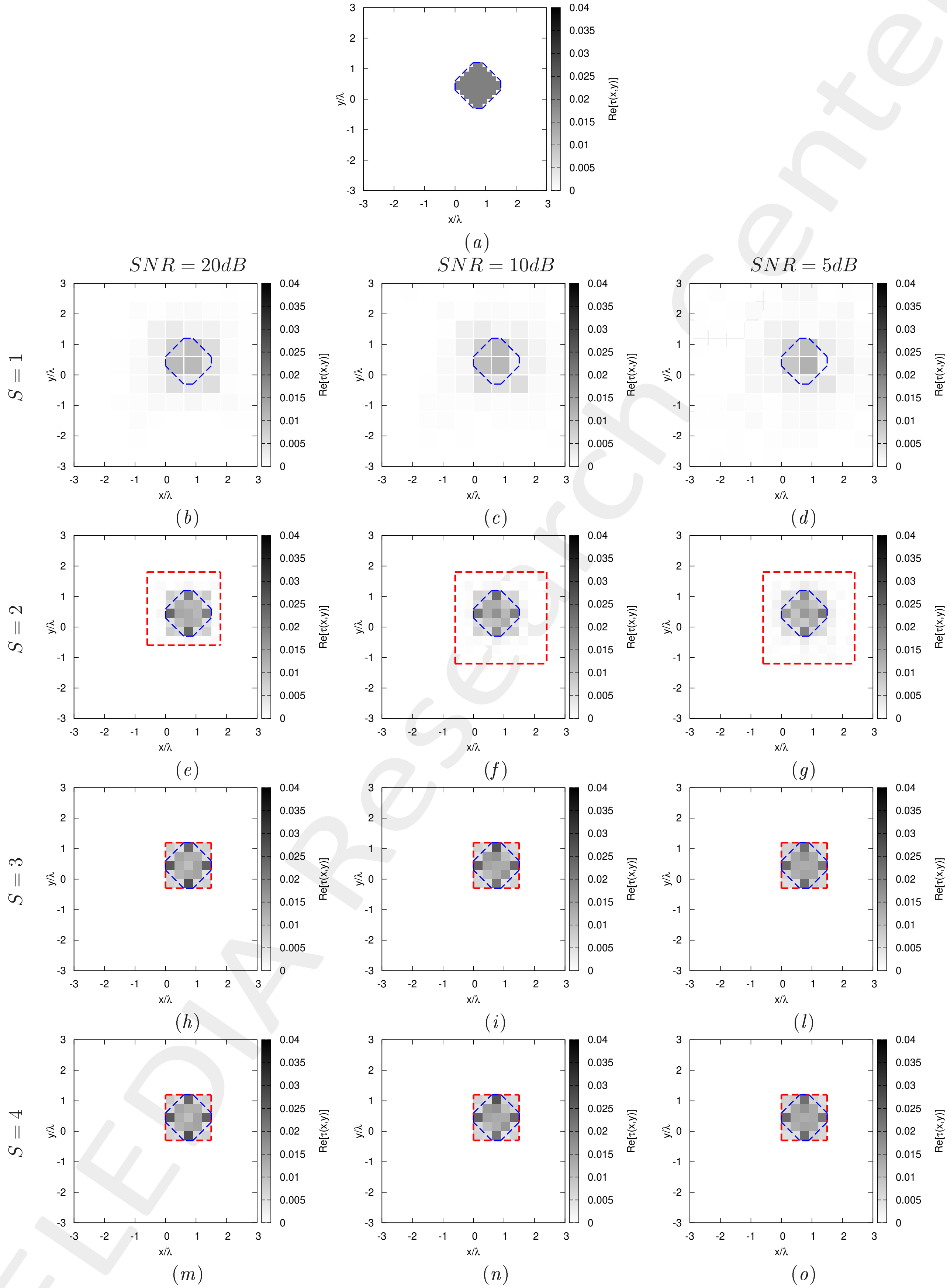

Figure 1: *Rhombus*, $D = 1.5\lambda$, $\tau = 0.02$ - (a) Actual profile and (b)-(o) IMSA-BCS reconstructed profiles for $(b)(e)(h)(m)$ $SNR = 20$ [dB], $(c)(f)(i)(n)$ $SNR = 10$ [dB] and $(d)(g)(l)(o)$ $SNR = 5$ [dB] at the step (b)-(d) $S = 1$, (e)-(g) $S = 2$, (h)-(l) $S = 3$ and (m)-(o) $S = 4$.

	$SNR = 50dB$			
	$S = 1$	$S = 2$	$S = 3$	$S = 4$
ξ_{tot}	1.05×10^{-3}	4.63×10^{-4}	4.48×10^{-4}	4.48×10^{-4}
ξ_{int}	1.09×10^{-2}	7.65×10^{-3}	7.80×10^{-3}	7.80×10^{-3}
ξ_{ext}	6.69×10^{-4}	1.82×10^{-4}	1.62×10^{-4}	1.62×10^{-4}
	$SNR = 20dB$			
	$S = 1$	$S = 2$	$S = 3$	$S = 4$
ξ_{tot}	1.05×10^{-3}	4.66×10^{-4}	4.44×10^{-4}	4.44×10^{-4}
ξ_{int}	1.08×10^{-2}	7.19×10^{-3}	7.59×10^{-3}	7.59×10^{-3}
ξ_{ext}	6.65×10^{-4}	2.03×10^{-4}	1.66×10^{-4}	1.66×10^{-4}
	$SNR = 10dB$			
	$S = 1$	$S = 2$	$S = 3$	$S = 4$
ξ_{tot}	1.09×10^{-3}	4.87×10^{-4}	4.04×10^{-4}	4.04×10^{-4}
ξ_{int}	1.08×10^{-2}	7.14×10^{-3}	6.67×10^{-3}	6.67×10^{-3}
ξ_{ext}	6.99×10^{-4}	2.26×10^{-4}	1.59×10^{-4}	1.59×10^{-4}
	$SNR = 5dB$			
	$S = 1$	$S = 2$	$S = 3$	$S = 4$
ξ_{tot}	1.18×10^{-3}	5.45×10^{-4}	3.88×10^{-4}	3.88×10^{-4}
ξ_{int}	1.10×10^{-2}	7.40×10^{-3}	6.03×10^{-3}	6.03×10^{-3}
ξ_{ext}	7.48×10^{-4}	2.71×10^{-4}	1.67×10^{-4}	1.67×10^{-4}

Table I: *Rhombus*, $D = 1.5\lambda$, $\tau = 0.20$ - Reconstruction errors: total (ξ_{tot}), internal (ξ_{int}) and external (ξ_{ext}) errors.

	$SNR = 50dB$			
	$S = 1$	$S = 2$	$S = 3$	$S = 4$
$L^{(S)}$	6.00	2.40	1.50	1.50
$N^{(S)}$	100	148	148	148
$Q^{(S)}$	100	64	25	25
	$SNR = 20dB$			
	$S = 1$	$S = 2$	$S = 3$	$S = 4$
$L^{(S)}$	6.00	2.40	1.50	1.50
$N^{(S)}$	100	148	148	148
$Q^{(S)}$	100	64	25	25
	$SNR = 10dB$			
	$S = 1$	$S = 2$	$S = 3$	$S = 4$
$L^{(S)}$	6.00	3.00	1.50	1.50
$N^{(S)}$	100	175	175	175
$Q^{(S)}$	100	100	25	25
	$SNR = 5dB$			
	$S = 1$	$S = 2$	$S = 3$	$S = 4$
$L^{(S)}$	6.00	3.00	1.50	1.50
$N^{(S)}$	100	175	175	175
$Q^{(S)}$	100	100	25	25

Table II: *Rhombus*, $D = 1.5\lambda$, $\tau = 0.02$ - Investigation domain parameters: restricted investigation domain size $L^{(S)}$, total number of cells $N^{(S)}$ and number of cells within the restricted domain size $Q^{(S)}$.

1.1.2 Rhombus, $D = 1.5\lambda$, $\tau = 0.05$ - IMSA-BCS reconstructed profiles

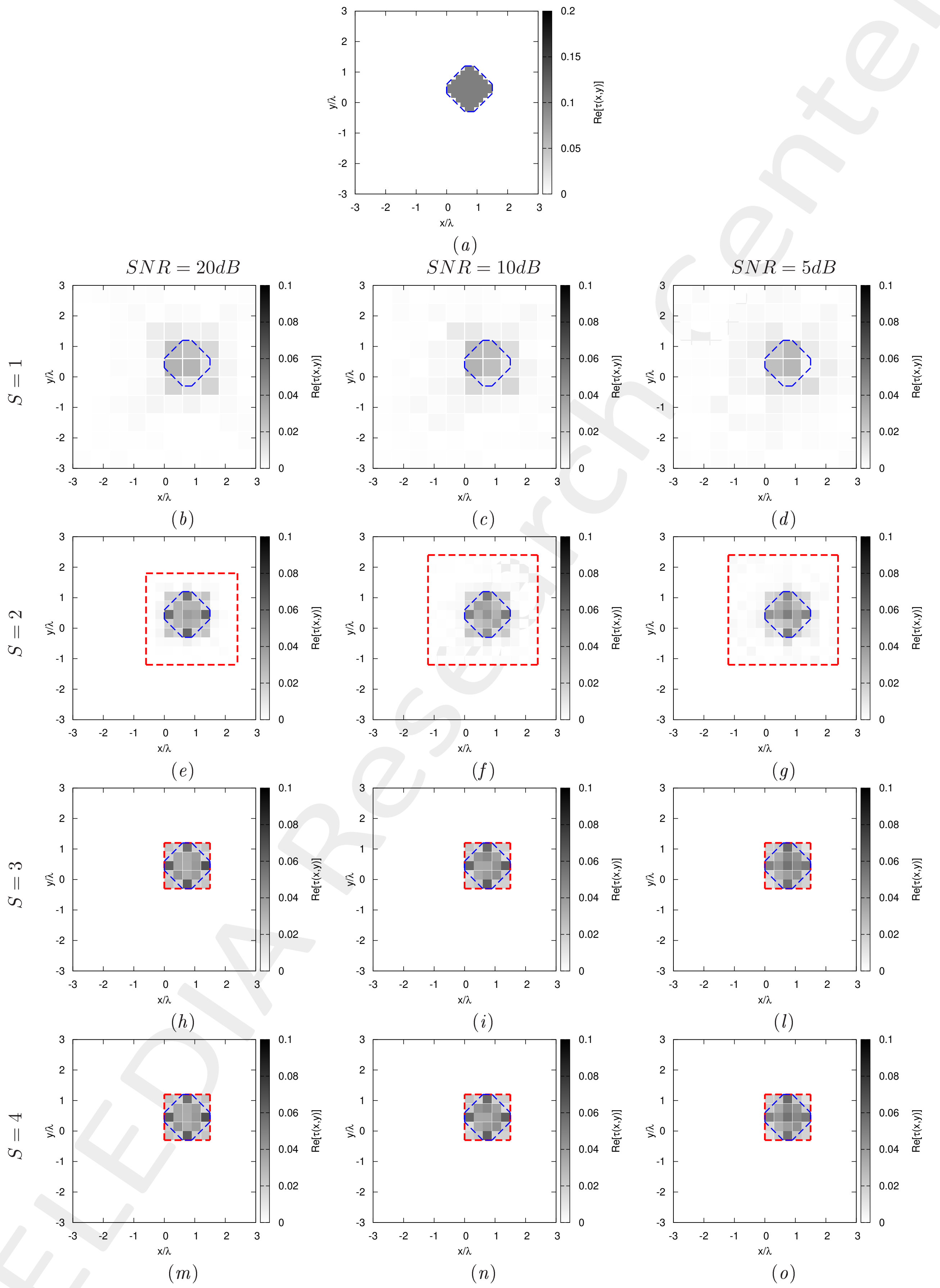

Figure 2: *Rhombus*, $D = 1.5\lambda$, $\tau = 0.05$ - (a) Actual profile and (b)-(o) IMSA-BCS reconstructed profiles for $(b)(e)(h)(m)$ $SNR = 20$ [dB], $(c)(f)(i)(n)$ $SNR = 10$ [dB] and $(d)(g)(l)(o)$ $SNR = 5$ [dB] at the step (b)-(d) $S = 1$, (e)-(g) $S = 2$, (h)-(l) $S = 3$ and (m)-(o) $S = 4$.

	$SNR = 50dB$			
	$S = 1$	$S = 2$	$S = 3$	$S = 4$
ξ_{tot}	3.01×10^{-3}	1.35×10^{-3}	1.12×10^{-3}	1.12×10^{-3}
ξ_{int}	2.39×10^{-2}	1.75×10^{-2}	1.65×10^{-2}	1.65×10^{-2}
ξ_{ext}	2.12×10^{-3}	6.98×10^{-4}	5.13×10^{-4}	5.13×10^{-4}
	$SNR = 20dB$			
	$S = 1$	$S = 2$	$S = 3$	$S = 4$
ξ_{tot}	3.04×10^{-3}	1.31×10^{-3}	1.09×10^{-3}	1.09×10^{-3}
ξ_{int}	2.45×10^{-2}	1.69×10^{-2}	1.53×10^{-2}	1.53×10^{-2}
ξ_{ext}	2.12×10^{-3}	6.81×10^{-4}	5.27×10^{-4}	5.27×10^{-4}
	$SNR = 10dB$			
	$S = 1$	$S = 2$	$S = 3$	$S = 4$
ξ_{tot}	3.12×10^{-3}	1.39×10^{-3}	9.67×10^{-4}	9.67×10^{-4}
ξ_{int}	2.51×10^{-2}	1.53×10^{-2}	1.30×10^{-2}	1.30×10^{-2}
ξ_{ext}	2.14×10^{-3}	7.93×10^{-4}	4.81×10^{-4}	4.81×10^{-4}
	$SNR = 5dB$			
	$S = 1$	$S = 2$	$S = 3$	$S = 4$
ξ_{tot}	3.30×10^{-3}	1.48×10^{-3}	8.71×10^{-4}	8.71×10^{-4}
ξ_{int}	2.61×10^{-2}	1.50×10^{-2}	1.01×10^{-2}	1.01×10^{-2}
ξ_{ext}	2.27×10^{-3}	8.39×10^{-4}	4.74×10^{-4}	4.74×10^{-4}

Table III: *Rhombus*, $D = 1.5\lambda$, $\tau = 0.20$ - Reconstruction errors: total (ξ_{tot}), internal (ξ_{int}) and external (ξ_{ext}) errors.

	$SNR = 50dB$			
	$S = 1$	$S = 2$	$S = 3$	$S = 4$
$L^{(S)}$	6.00	3.00	1.50	1.50
$N^{(S)}$	100	175	175	175
$Q^{(S)}$	100	100	25	25
	$SNR = 20dB$			
	$S = 1$	$S = 2$	$S = 3$	$S = 4$
$L^{(S)}$	6.00	3.00	1.50	1.50
$N^{(S)}$	100	175	175	175
$Q^{(S)}$	100	100	25	25
	$SNR = 10dB$			
	$S = 1$	$S = 2$	$S = 3$	$S = 4$
$L^{(S)}$	6.00	3.60	1.50	1.50
$N^{(S)}$	100	208	208	208
$Q^{(S)}$	100	144	25	25
	$SNR = 5dB$			
	$S = 1$	$S = 2$	$S = 3$	$S = 4$
$L^{(S)}$	6.00	3.60	1.50	1.50
$N^{(S)}$	100	208	208	208
$Q^{(S)}$	100	144	25	25

Table IV: *Rhombus*, $D = 1.5\lambda$, $\tau = 0.05$ - Investigation domain parameters: restricted investigation domain size $L^{(S)}$, total number of cells $N^{(S)}$ and number of cells within the restricted domain size $Q^{(S)}$.

1.1.3 Rhombus, $D = 1.5\lambda$, $\tau = 0.10$ - IMSA-BCS reconstructed profiles

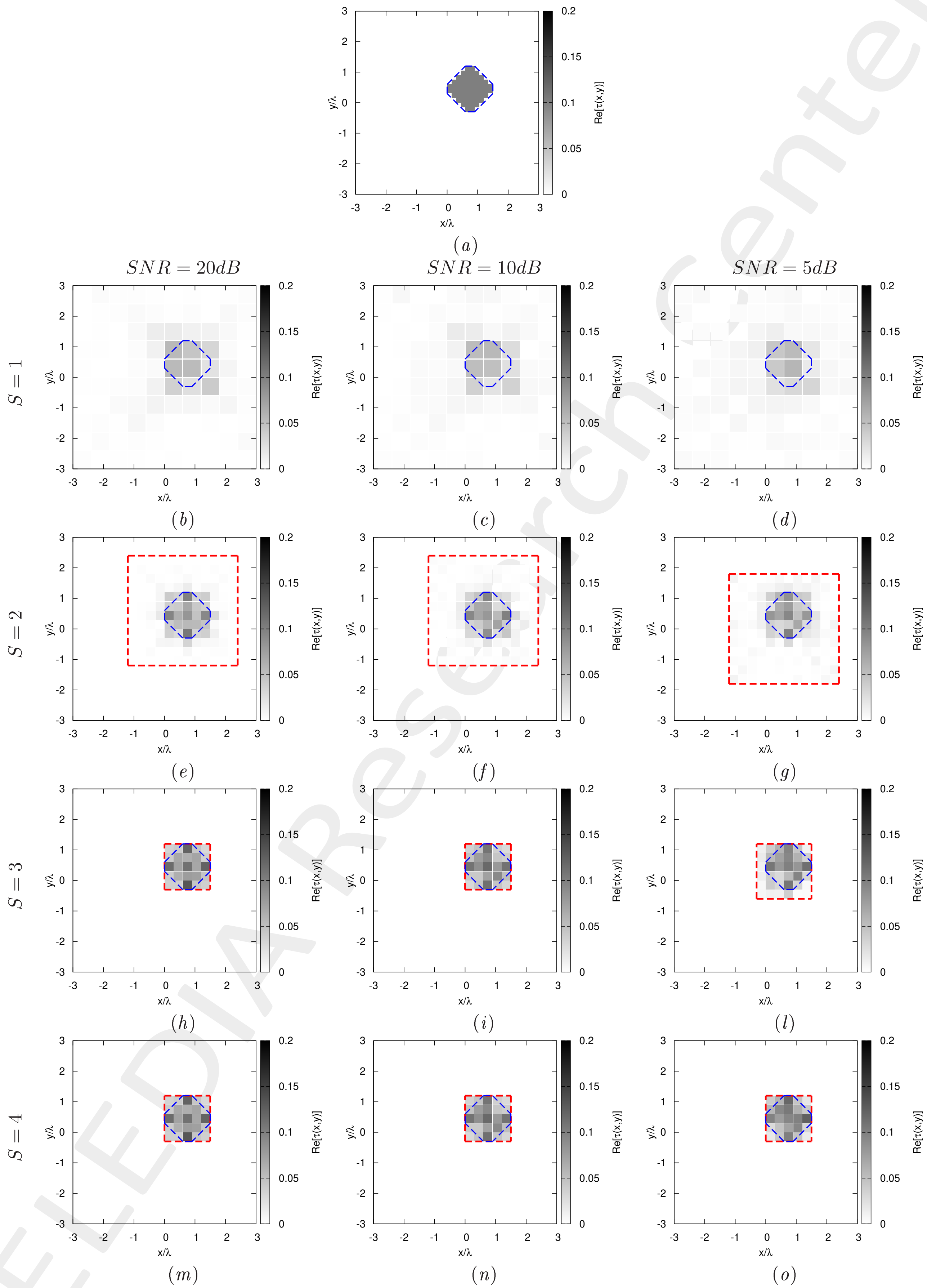

Figure 3: *Rhombus*, $D = 1.5\lambda$, $\tau = 0.10$ - (a) Actual profile and (b)-(o) IMSA-BCS reconstructed profiles for $(b)(e)(h)$ $SNR = 20$ [dB], $(c)(f)(i)$ $SNR = 10$ [dB] and $(d)(g)(l)$ $SNR = 5$ [dB] at the step (b)-(d) $S = 1$, (e)-(g) $S = 2$, and (h)-(l) $S = 3$.

	$SNR = 50dB$			
	$S=1$	$S=2$	$S=3$	$S=4$
ξ_{tot}	6.37×10^{-3}	3.09×10^{-3}	2.10×10^{-3}	2.10×10^{-3}
ξ_{int}	4.77×10^{-2}	3.29×10^{-2}	2.72×10^{-2}	2.72×10^{-2}
ξ_{ext}	4.40×10^{-3}	1.73×10^{-3}	9.86×10^{-4}	9.86×10^{-4}
	$SNR = 20dB$			
	$S=1$	$S=2$	$S=3$	$S=4$
ξ_{tot}	6.52×10^{-3}	3.08×10^{-3}	2.18×10^{-3}	2.18×10^{-3}
ξ_{int}	4.86×10^{-2}	3.27×10^{-2}	2.81×10^{-2}	2.81×10^{-2}
ξ_{ext}	4.48×10^{-3}	1.71×10^{-3}	1.01×10^{-3}	1.01×10^{-3}
	$SNR = 10dB$			
	$S=1$	$S=2$	$S=3$	$S=4$
ξ_{tot}	6.51×10^{-3}	3.14×10^{-3}	2.05×10^{-3}	2.05×10^{-3}
ξ_{int}	4.86×10^{-2}	3.10×10^{-2}	2.29×10^{-2}	2.29×10^{-2}
ξ_{ext}	4.46×10^{-3}	1.76×10^{-3}	1.02×10^{-3}	1.02×10^{-3}
	$SNR = 5dB$			
	$S=1$	$S=2$	$S=3$	$S=4$
ξ_{tot}	7.15×10^{-3}	3.65×10^{-3}	2.40×10^{-3}	1.88×10^{-3}
ξ_{int}	5.01×10^{-2}	3.35×10^{-2}	2.29×10^{-2}	1.95×10^{-2}
ξ_{ext}	4.84×10^{-3}	2.11×10^{-3}	1.22×10^{-3}	9.40×10^{-4}

Table V: *Rhombus*, $D = 1.5\lambda$, $\tau = 0.20$ - Reconstruction errors: total (ξ_{tot}), internal (ξ_{int}) and external (ξ_{ext}) errors.

	$SNR = 50dB$			
	$S=1$	$S=2$	$S=3$	$S=4$
$L^{(S)}$	6.00	3.60	1.50	1.50
$N^{(S)}$	100	208	208	208
$Q^{(S)}$	100	144	25	25
	$SNR = 20dB$			
	$S=1$	$S=2$	$S=3$	$S=4$
$L^{(S)}$	6.00	3.60	1.50	1.50
$N^{(S)}$	100	208	208	208
$Q^{(S)}$	100	144	25	25
	$SNR = 10dB$			
	$S=1$	$S=2$	$S=3$	$S=4$
$L^{(S)}$	6.00	3.60	1.50	1.50
$N^{(S)}$	100	208	208	208
$Q^{(S)}$	100	144	25	25
	$SNR = 5dB$			
	$S=1$	$S=2$	$S=3$	$S=4$
$L^{(S)}$	6.00	3.60	1.80	1.50
$N^{(S)}$	100	208	208	208
$Q^{(S)}$	100	144	36	25

Table VI: *Rhombus*, $D = 1.5\lambda$, $\tau = 0.05$ - Investigation domain parameters: restricted investigation domain size $L^{(S)}$, total number of cells $N^{(S)}$ and number of cells within the restricted domain size $Q^{(S)}$.

1.1.4 Rhombus, $D = 1.5\lambda$, $\tau = 0.15$ - IMSA-BCS reconstructed profiles

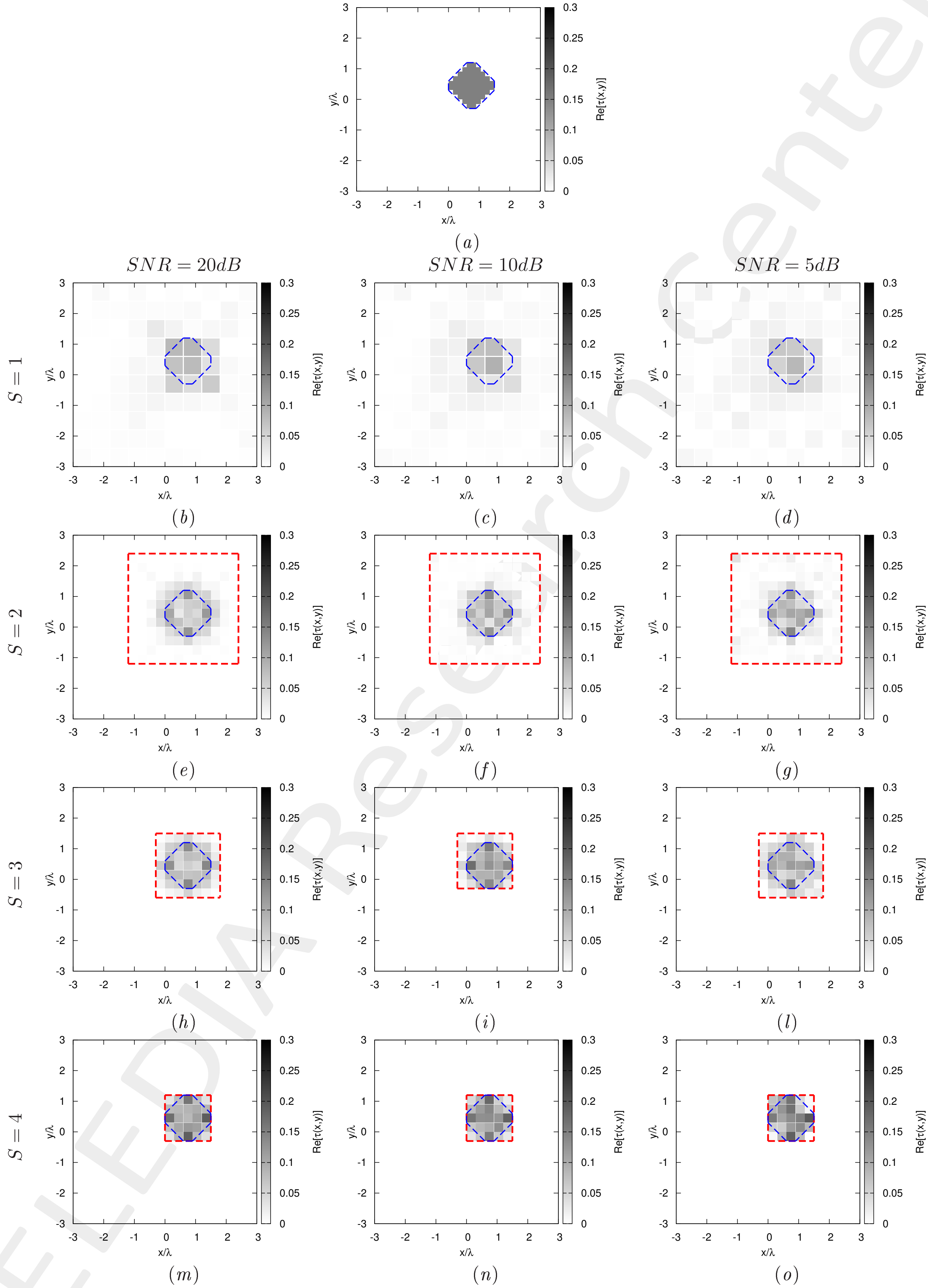

Figure 4: *Rhombus*, $D = 1.5\lambda$, $\tau = 0.15$ - (a) Actual profile and (b)-(o) IMSA-BCS reconstructed profiles for $(b)(e)(h)$ $SNR = 20$ [dB], $(c)(f)(i)$ $SNR = 10$ [dB] and $(d)(g)(l)$ $SNR = 5$ [dB] at the step (b)-(d) $S = 1$, (e)-(g) $S = 2$, and (h)-(l) $S = 3$.

	$SNR = 50dB$			
	$S=1$	$S=2$	$S=3$	$S=4$
ξ_{tot}	9.65×10^{-3}	6.53×10^{-3}	5.42×10^{-3}	3.51×10^{-3}
ξ_{int}	6.97×10^{-2}	7.15×10^{-2}	6.00×10^{-2}	4.27×10^{-2}
ξ_{ext}	6.50×10^{-3}	3.64×10^{-3}	3.02×10^{-3}	1.52×10^{-3}
	$SNR = 20dB$			
	$S=1$	$S=2$	$S=3$	$S=4$
ξ_{tot}	9.72×10^{-3}	6.42×10^{-3}	5.35×10^{-3}	3.53×10^{-3}
ξ_{int}	6.83×10^{-2}	6.85×10^{-2}	5.81×10^{-2}	4.09×10^{-2}
ξ_{ext}	6.63×10^{-3}	3.54×10^{-3}	2.96×10^{-3}	1.62×10^{-3}
	$SNR = 10dB$			
	$S=1$	$S=2$	$S=3$	$S=4$
ξ_{tot}	9.95×10^{-3}	5.75×10^{-3}	3.91×10^{-3}	3.06×10^{-3}
ξ_{int}	7.07×10^{-2}	5.83×10^{-2}	3.94×10^{-2}	3.18×10^{-2}
ξ_{ext}	6.81×10^{-3}	3.14×10^{-3}	2.01×10^{-3}	1.38×10^{-3}
	$SNR = 5dB$			
	$S=1$	$S=2$	$S=3$	$S=4$
ξ_{tot}	1.25×10^{-2}	6.78×10^{-3}	5.43×10^{-3}	3.39×10^{-3}
ξ_{int}	7.61×10^{-2}	5.72×10^{-2}	5.37×10^{-2}	3.40×10^{-2}
ξ_{ext}	8.33×10^{-3}	3.72×10^{-3}	3.07×10^{-3}	1.32×10^{-3}

Table VII: *Rhombus*, $D = 1.5\lambda$, $\tau = 0.20$ - Reconstruction errors: total (ξ_{tot}), internal (ξ_{int}) and external (ξ_{ext}) errors.

	$SNR = 50dB$			
	$S=1$	$S=2$	$S=3$	$S=4$
$L^{(S)}$	6.00	3.60	2.10	1.50
$N^{(S)}$	100	208	208	208
$Q^{(S)}$	100	144	49	25
	$SNR = 20dB$			
	$S=1$	$S=2$	$S=3$	$S=4$
$L^{(S)}$	6.00	3.60	2.10	1.50
$N^{(S)}$	100	208	208	208
$Q^{(S)}$	100	144	49	25
	$SNR = 10dB$			
	$S=1$	$S=2$	$S=3$	$S=4$
$L^{(S)}$	6.00	3.60	1.80	1.50
$N^{(S)}$	100	208	208	208
$Q^{(S)}$	100	144	36	25
	$SNR = 5dB$			
	$S=1$	$S=2$	$S=3$	$S=4$
$L^{(S)}$	6.00	3.60	2.10	1.50
$N^{(S)}$	100	208	208	208
$Q^{(S)}$	100	144	49	25

Table VIII: *Rhombus*, $D = 1.5\lambda$, $\tau = 0.05$ - Investigation domain parameters: restricted investigation domain size $L^{(S)}$, total number of cells $N^{(S)}$ and number of cells within the restricted domain size $Q^{(S)}$.

1.1.5 Rhombus, $D = 1.5\lambda$, $\tau = 0.20$ - IMSA-BCS reconstructed profiles

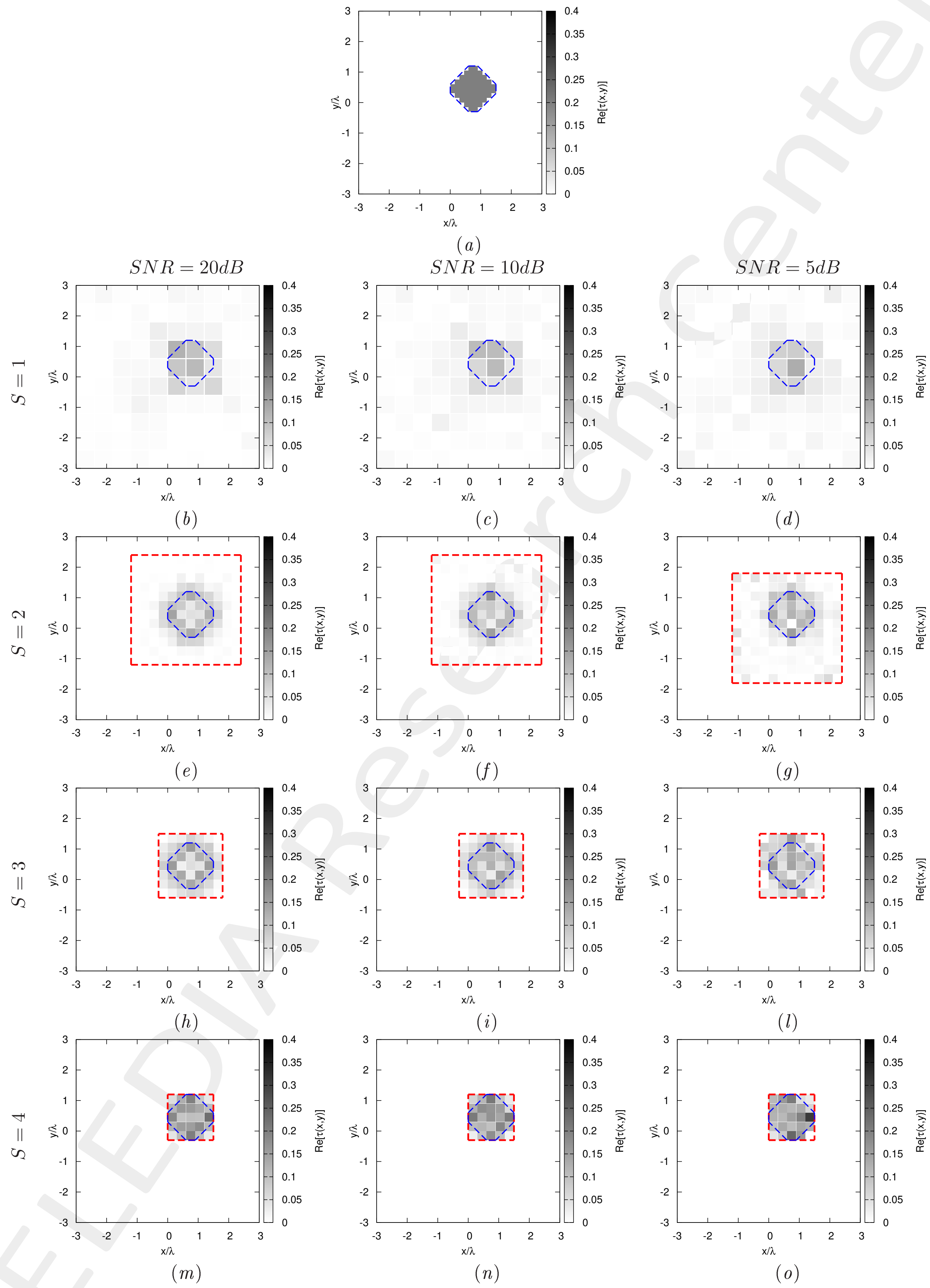

Figure 5: *Rhombus*, $D = 1.5\lambda$, $\tau = 0.20$ - (a) Actual profile and (b)-(o) IMSA-BCS reconstructed profiles for $(b)(e)(h)$ $SNR = 20$ [dB], $(c)(f)(i)$ $SNR = 10$ [dB] and $(d)(g)(l)$ $SNR = 5$ [dB] at the step (b)-(d) $S = 1$, (e)-(g) $S = 2$, and (h)-(l) $S = 3$.

	$SNR = 50dB$			
	$S=1$	$S=2$	$S=3$	$S=4$
ξ_{tot}	1.29×10^{-2}	9.07×10^{-3}	7.31×10^{-3}	4.83×10^{-3}
ξ_{int}	9.23×10^{-2}	9.49×10^{-2}	7.80×10^{-2}	4.18×10^{-2}
ξ_{ext}	8.61×10^{-3}	4.89×10^{-3}	3.86×10^{-3}	2.16×10^{-3}
	$SNR = 20dB$			
	$S=1$	$S=2$	$S=3$	$S=4$
ξ_{tot}	1.31×10^{-2}	9.14×10^{-3}	7.67×10^{-3}	4.86×10^{-3}
ξ_{int}	9.19×10^{-2}	9.64×10^{-2}	8.29×10^{-2}	4.42×10^{-2}
ξ_{ext}	8.60×10^{-3}	4.92×10^{-3}	4.14×10^{-3}	2.13×10^{-3}
	$SNR = 10dB$			
	$S=1$	$S=2$	$S=3$	$S=4$
ξ_{tot}	1.45×10^{-2}	9.40×10^{-3}	7.98×10^{-3}	4.56×10^{-3}
ξ_{int}	9.64×10^{-2}	9.49×10^{-2}	8.43×10^{-2}	3.97×10^{-2}
ξ_{ext}	9.53×10^{-3}	5.01×10^{-3}	4.34×10^{-3}	1.95×10^{-3}
	$SNR = 5dB$			
	$S=1$	$S=2$	$S=3$	$S=4$
ξ_{tot}	1.84×10^{-2}	1.21×10^{-2}	9.75×10^{-3}	5.47×10^{-3}
ξ_{int}	9.86×10^{-2}	9.05×10^{-2}	8.26×10^{-2}	5.71×10^{-2}
ξ_{ext}	1.12×10^{-2}	6.90×10^{-3}	5.34×10^{-3}	2.22×10^{-3}

Table IX: *Rhombus*, $D = 1.5\lambda$, $\tau = 0.20$ - Reconstruction errors: total (ξ_{tot}), internal (ξ_{int}) and external (ξ_{ext}) errors.

	$SNR = 50dB$			
	$S=1$	$S=2$	$S=3$	$S=4$
$L^{(S)}$	6.00	3.60	2.10	1.50
$N^{(S)}$	100	208	208	208
$Q^{(S)}$	100	144	49	25
	$SNR = 20dB$			
	$S=1$	$S=2$	$S=3$	$S=4$
$L^{(S)}$	6.00	3.60	2.10	1.50
$N^{(S)}$	100	208	208	208
$Q^{(S)}$	100	144	49	25
	$SNR = 10dB$			
	$S=1$	$S=2$	$S=3$	$S=4$
$L^{(S)}$	6.00	3.60	2.10	1.50
$N^{(S)}$	100	208	208	208
$Q^{(S)}$	100	144	49	25
	$SNR = 5dB$			
	$S=1$	$S=2$	$S=3$	$S=4$
$L^{(S)}$	6.00	3.60	2.10	1.50
$N^{(S)}$	100	208	208	208
$Q^{(S)}$	100	144	49	25

Table X: *Rhombus*, $D = 1.5\lambda$, $\tau = 0.20$ - Investigation domain parameters: restricted investigation domain size $L^{(S)}$, total number of cells $N^{(S)}$ and number of cells within the restricted domain size $Q^{(S)}$.

1.1.6 Rhombus, $D = 1.5\lambda$, $\tau = 0.20$ - IMSA-BCS multi-resolution grids

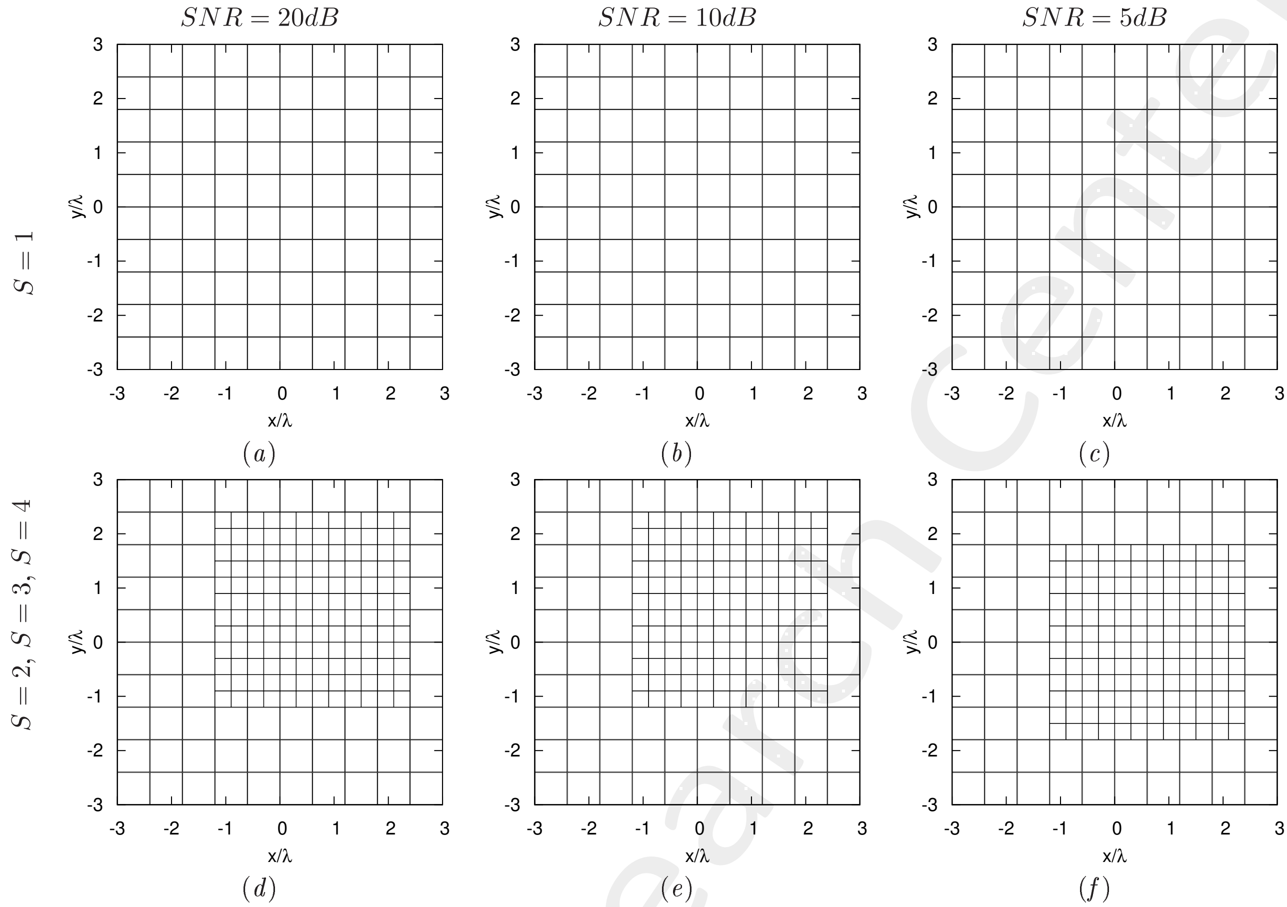

Figure 6: *Rhombus*, $D = 1.5\lambda$, $\tau = 0.20$ - Example of IMSA-BCS multi-resolution grids for $(a)(d)$ $SNR = 20$ [dB], $(b)(e)$ $SNR = 10$ [dB] and $(c)(f)$ $SNR = 5$ [dB] at the step (a)-(c) $S = 1$ and (d)-(f) $S = 2$, 3 4.

1.1.7 Rhombus, $D = 1.5\lambda$ - Resume: Errors vs. τ

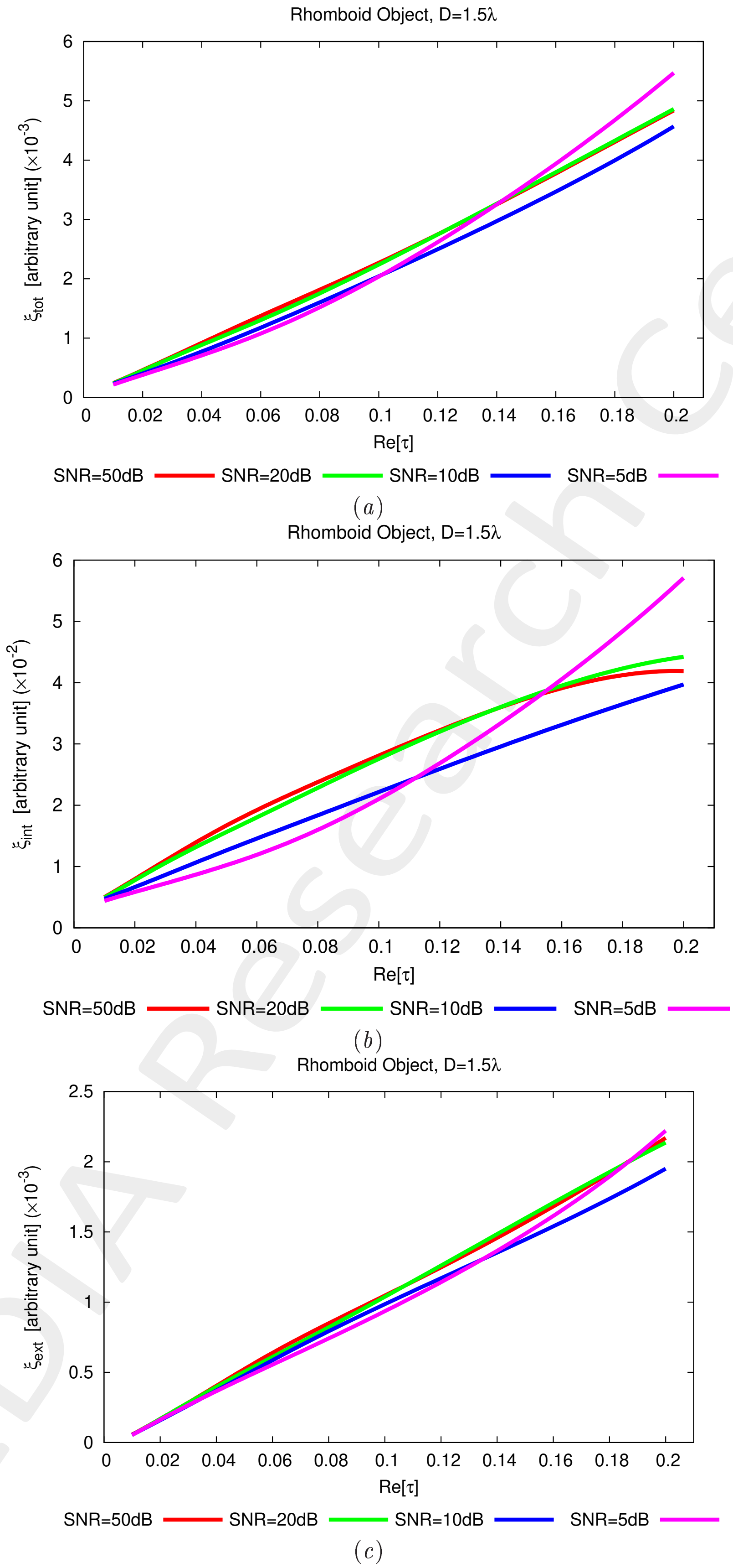

Figure 7: *Rhombus*, $D = 1.5\lambda$ - Reconstruction errors vs. τ: (a) total error, (b) internal error and (c) external error.

1.1.8 Rhombus, $D = 1.5\lambda$ - Resume: Errors vs. SNR

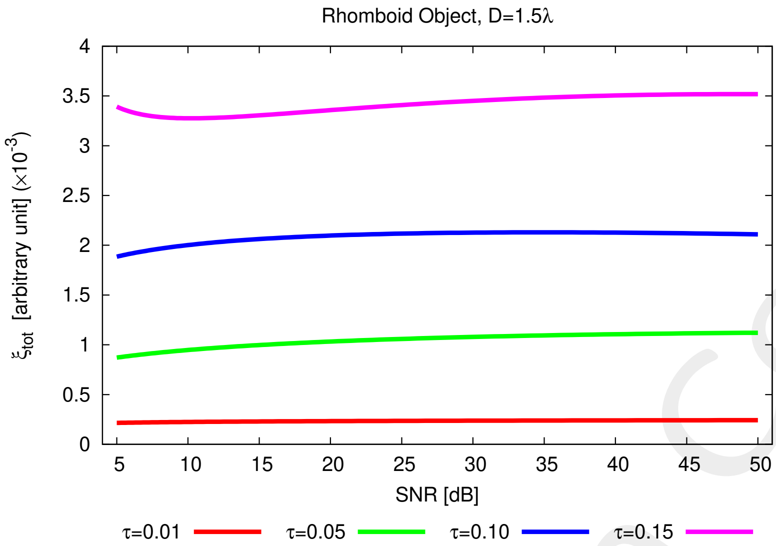

(a)

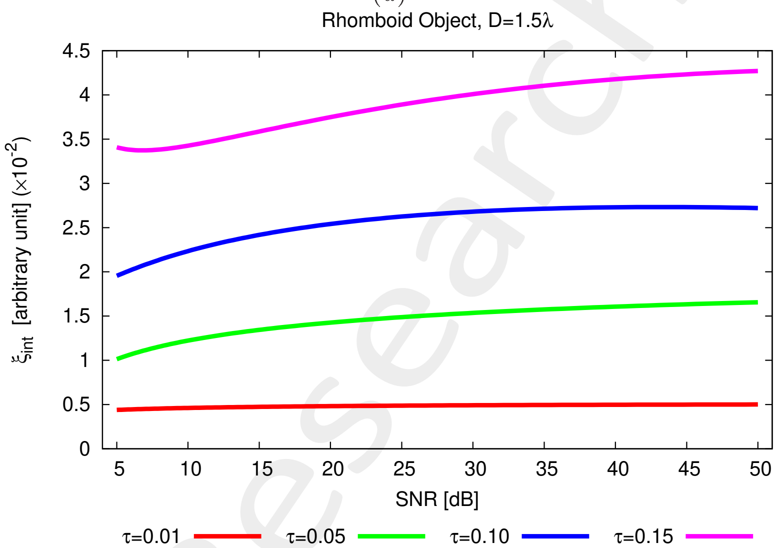

(b)

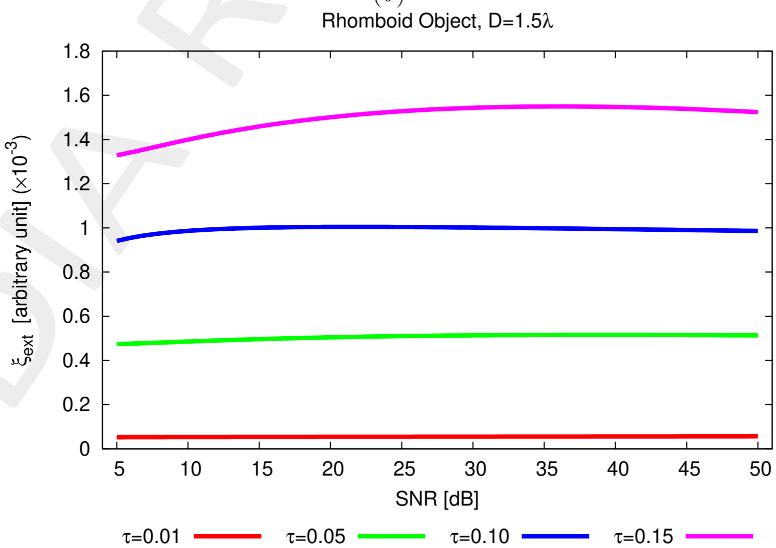

(c)

Figure 8: *Rhombus*, $D = 1.5\lambda$ - Reconstruction errors vs. SNR: (a) total error, (b) internal error and (c) external error.

1.1.9 Rhombus, $D = 1.5\lambda$ - Resume: Errors vs. $IMSA$ step, S

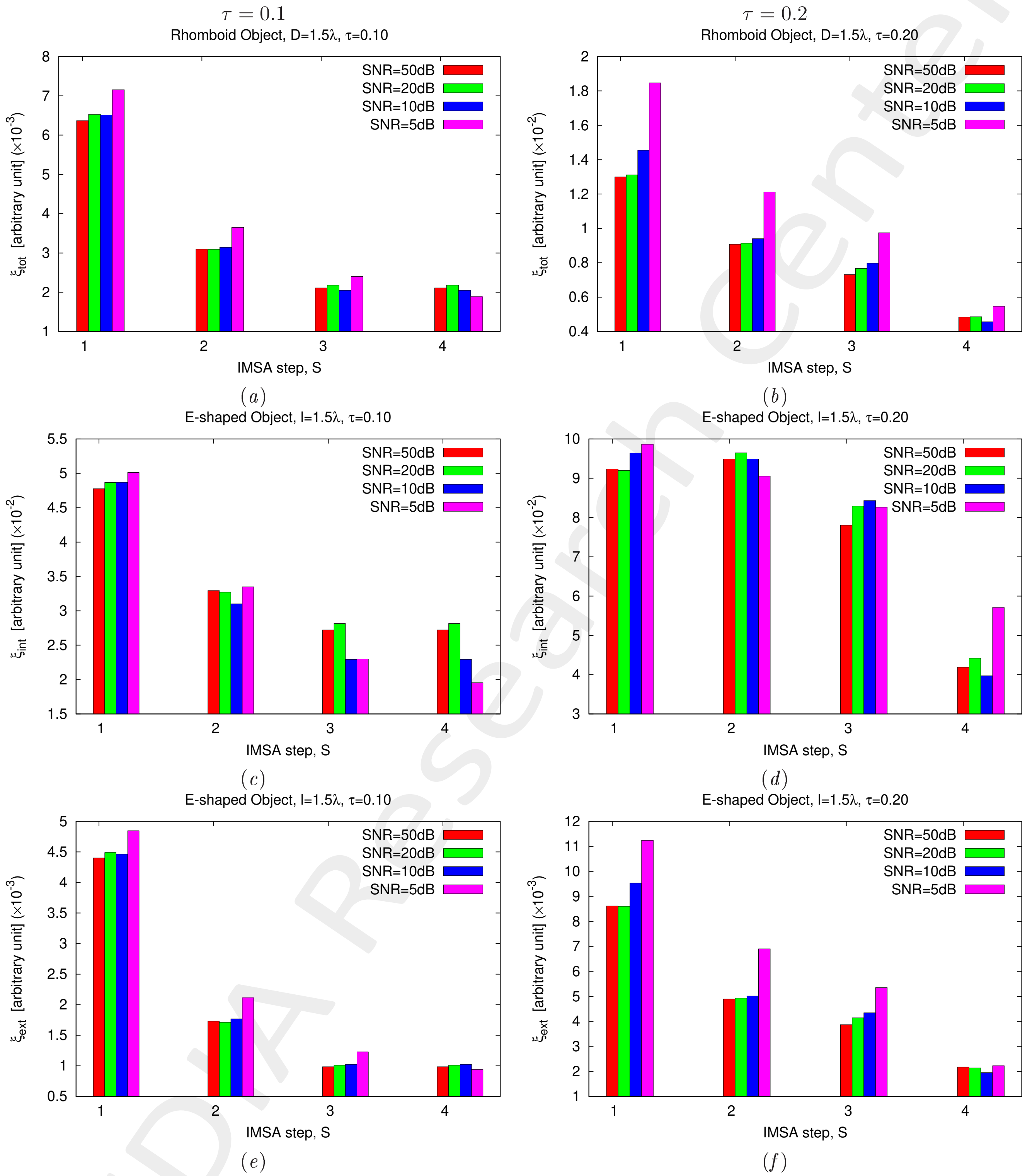

Figure 9: *Rhombus*, $D = 1.5\lambda$ - Reconstruction errors vs. $IMSA$ step, S: $(a)(b)$ total error, $(c)(d)$ internal error and $(e)(f)$ external error for $(a)(c)(e)$ $\tau = 0.1$ and $(b)(d)(f)$ $\tau = 0.2$.

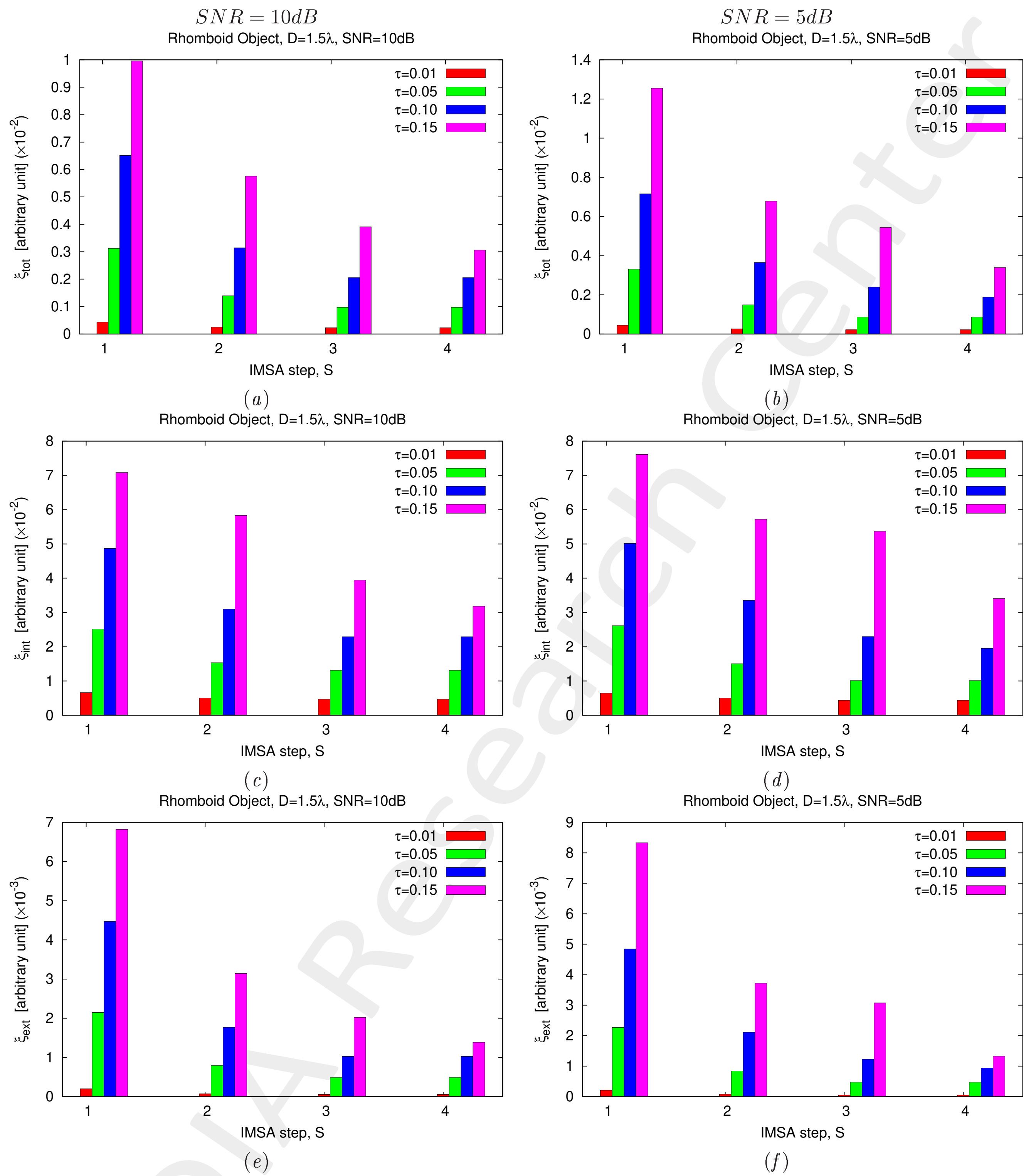

Figure 10: *Rhombus*, $D = 1.5\lambda$ - Reconstruction errors vs. $IMSA$ step, S: $(a)(b)$ total error, $(c)(d)$ internal error and $(e)(f)$ external error for $(a)(c)(e)$ $SNR = 10dB$ and $(b)(d)(f)$ $SNR = 5dB$.

1.2 Porous Object

Test Case Description

Direct solver:

- Side of the investigation domain: $L = 6.0\lambda$
- Cubic domain divided in $\sqrt{D} \times \sqrt{D}$ cells
- Number of cells for the direct solver: $D = 1600$ (discretization $= \lambda/10$)

Investigation domain:

- Cubic domain divided in $\sqrt{N} \times \sqrt{N}$ cells
- Number of cells for the inversion:
  - First Step IMSA: $N^{(1)} = 100$ (discretization $= \lambda/10$)
  - Following Steps IMSA: $N^{(i)}$ not fixed, defined according to the estimated *RoI* $\mathcal{D}^{(i)}$

Measurement domain:

- Total number of measurements: $M = 60$
- Measurement points placed on circles of radius $\rho = 4.5\lambda$

Sources:

- Plane waves
- Number of views: $V = 60$; $\theta_{inc}^{v} = 0° + (v-1) \times (360/V)$
- Amplitude: $A = 1.0$
- Frequency: $F = 300$ MHz ($\lambda = 1$)

Background:

- $\varepsilon_r = 1.0$
- $\sigma = 0$ [S/m]

Scatterer

- Porous object
- $\varepsilon_r \in \{1.01, 1.02, 1.04, 1.05, 1.06, 1.08, 1.10, 1.15, 1.20\}$
- $\sigma = 0$ [S/m]

1.2.1 Porous Object, $\ell = 1.5\lambda$, $\tau = 0.02$ - IMSA-BCS reconstructed profiles

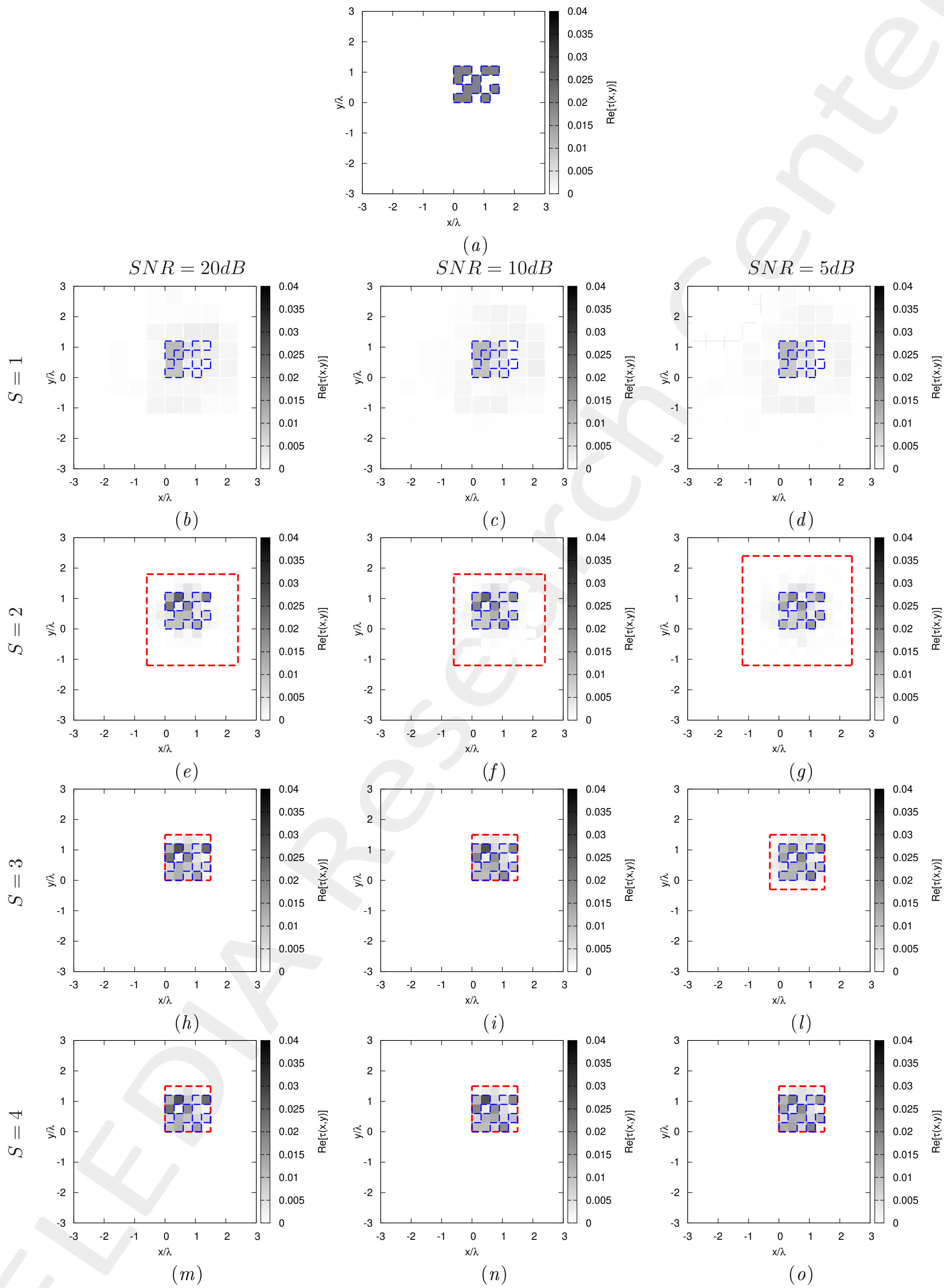

Figure 11: *Porous Object*, $\tau = 0.02$ - (a) Actual profile and (b)-(o) IMSA-BCS reconstructed profiles for $(b)(e)(h)(m)$ $SNR = 20$ [dB], $(c)(f)(i)(n)$ $SNR = 10$ [dB] and $(d)(g)(l)(o)$ $SNR = 5$ [dB] at the step (b)-(d) $S = 1$, (e)-(g) $S = 2$, (h)-(l) $S = 3$ and (m)-(o) $S = 4$.

	$SNR = 50dB$			
	$S=1$	$S=2$	$S=3$	$S=4$
ξ_{tot}	8.60×10^{-4}	3.52×10^{-4}	3.21×10^{-4}	3.21×10^{-4}
ξ_{int}	1.27×10^{-2}	7.39×10^{-3}	7.20×10^{-3}	7.20×10^{-3}
ξ_{ext}	4.88×10^{-4}	1.34×10^{-4}	1.08×10^{-4}	1.08×10^{-4}
	$SNR = 20dB$			
	$S=1$	$S=2$	$S=3$	$S=4$
ξ_{tot}	8.73×10^{-4}	3.73×10^{-4}	3.41×10^{-4}	3.41×10^{-4}
ξ_{int}	1.29×10^{-2}	7.61×10^{-3}	7.59×10^{-3}	7.59×10^{-3}
ξ_{ext}	4.96×10^{-4}	1.49×10^{-4}	1.16×10^{-4}	1.16×10^{-4}
	$SNR = 10dB$			
	$S=1$	$S=2$	$S=3$	$S=4$
ξ_{tot}	8.87×10^{-4}	3.79×10^{-4}	3.19×10^{-4}	3.19×10^{-4}
ξ_{int}	1.28×10^{-2}	7.40×10^{-3}	6.82×10^{-3}	6.82×10^{-3}
ξ_{ext}	5.11×10^{-4}	1.61×10^{-4}	1.18×10^{-4}	1.18×10^{-4}
	$SNR = 5dB$			
	$S=1$	$S=2$	$S=3$	$S=4$
ξ_{tot}	9.44×10^{-4}	4.50×10^{-4}	3.40×10^{-4}	2.89×10^{-4}
ξ_{int}	1.30×10^{-2}	8.14×10^{-3}	6.39×10^{-3}	5.67×10^{-3}
ξ_{ext}	5.54×10^{-4}	2.08×10^{-4}	1.51×10^{-4}	1.22×10^{-4}

Table XI: *Porous Object*, $\tau = 0.02$ - Reconstruction errors: total (ξ_{tot}), internal (ξ_{int}) and external (ξ_{ext}) errors.

	$SNR = 50dB$			
	$S=1$	$S=2$	$S=3$	$S=4$
$L^{(S)}$	6.00	1.50	1.50	1.50
$N^{(S)}$	100	175	175	175
$Q^{(S)}$	100	100	25	25
	$SNR = 20dB$			
	$S=1$	$S=2$	$S=3$	$S=4$
$L^{(S)}$	6.00	1.50	1.50	1.50
$N^{(S)}$	100	175	175	175
$Q^{(S)}$	100	100	25	25
	$SNR = 10dB$			
	$S=1$	$S=2$	$S=3$	$S=4$
$L^{(S)}$	6.00	1.50	1.50	1.50
$N^{(S)}$	100	175	175	175
$Q^{(S)}$	100	100	25	25
	$SNR = 5dB$			
	$S=1$	$S=2$	$S=3$	$S=4$
$L^{(S)}$	6.00	1.50	1.50	1.50
$N^{(S)}$	100	208	208	208
$Q^{(S)}$	100	144	36	25

Table XII: *Porous Object*, $\tau = 0.02$ - Investigation domain parameters: restricted investigation domain size $L^{(S)}$, total number of cells $N^{(S)}$ and number of cells within the restricted domain size $Q^{(S)}$.

1.2.2 Porous Object, $\ell = 1.5\lambda$, $\tau = 0.05$ - IMSA-BCS reconstructed profiles

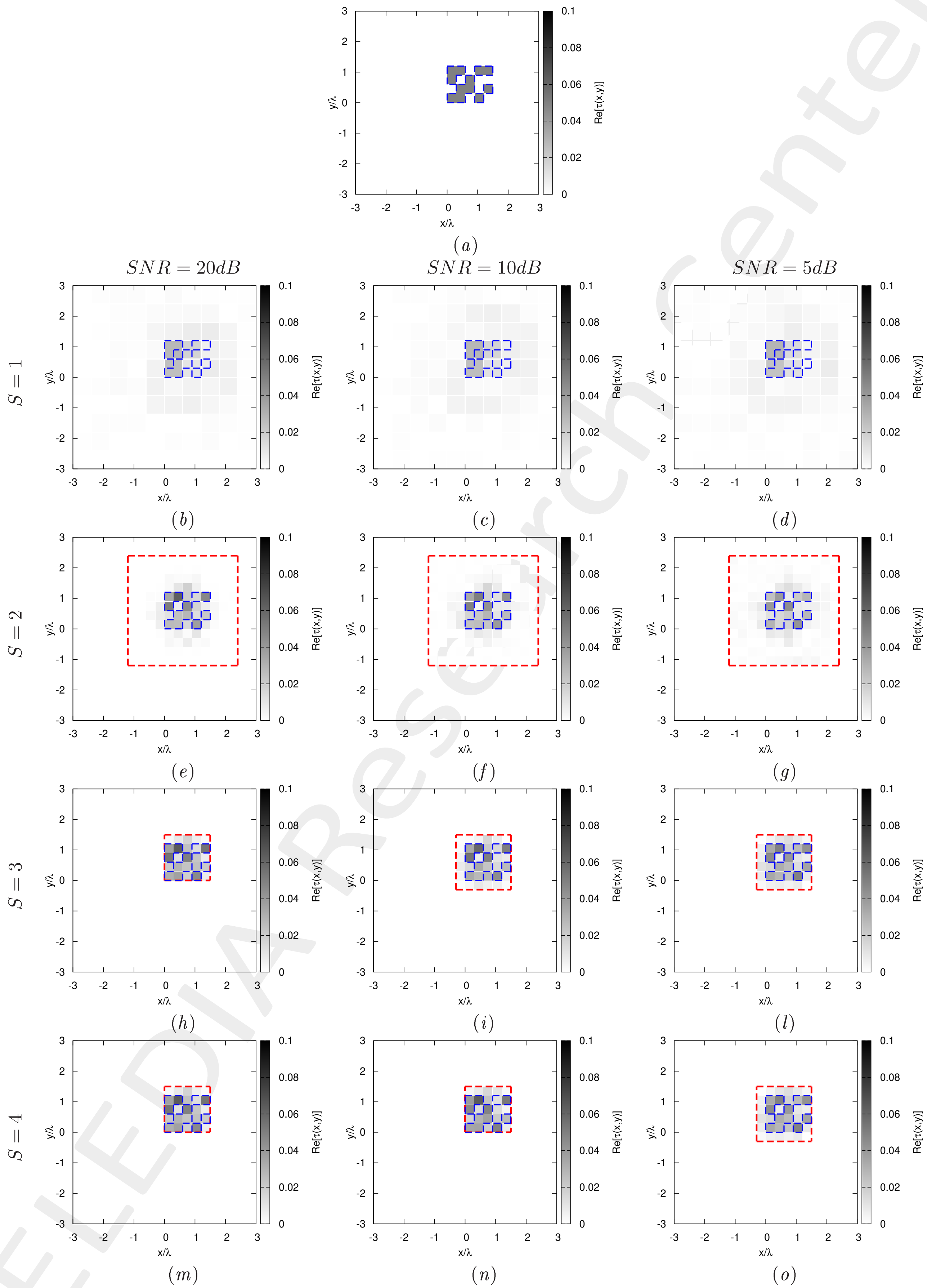

Figure 12: *Porous Object*, $\tau = 0.05$ - (a) Actual profile and (b)-(o) IMSA-BCS reconstructed profiles for $(b)(e)(h)(m)$ $SNR = 20$ [dB], $(c)(f)(i)(n)$ $SNR = 10$ [dB] and $(d)(g)(l)(o)$ $SNR = 5$ [dB] at the step (b)-(d) $S = 1$, (e)-(g) $S = 2$, (h)-(l) $S = 3$ and (m)-(o) $S = 4$.

	$SNR = 50dB$			
	$S=1$	$S=2$	$S=3$	$S=4$
ξ_{tot}	2.64×10^{-3}	1.08×10^{-3}	9.33×10^{-4}	8.96×10^{-4}
ξ_{int}	2.94×10^{-2}	1.69×10^{-2}	1.57×10^{-2}	1.50×10^{-2}
ξ_{ext}	1.76×10^{-3}	5.81×10^{-4}	4.68×10^{-4}	4.49×10^{-4}
	$SNR = 20dB$			
	$S=1$	$S=2$	$S=3$	$S=4$
ξ_{tot}	2.67×10^{-3}	1.07×10^{-3}	8.87×10^{-4}	8.87×10^{-4}
ξ_{int}	2.95×10^{-2}	1.65×10^{-2}	1.47×10^{-2}	1.47×10^{-2}
ξ_{ext}	1.78×10^{-3}	5.81×10^{-4}	4.51×10^{-4}	4.51×10^{-4}
	$SNR = 10dB$			
	$S=1$	$S=2$	$S=3$	$S=4$
ξ_{tot}	2.68×10^{-3}	1.13×10^{-3}	9.14×10^{-4}	7.91×10^{-4}
ξ_{int}	2.91×10^{-2}	1.61×10^{-2}	1.40×10^{-2}	1.26×10^{-2}
ξ_{ext}	1.78×10^{-3}	6.30×10^{-4}	4.89×10^{-4}	4.14×10^{-4}
	$SNR = 5dB$			
	$S=1$	$S=2$	$S=3$	$S=4$
ξ_{tot}	2.84×10^{-3}	1.42×10^{-3}	8.95×10^{-4}	8.95×10^{-4}
ξ_{int}	3.00×10^{-2}	2.00×10^{-2}	1.25×10^{-2}	1.25×10^{-2}
ξ_{ext}	1.88×10^{-3}	7.89×10^{-4}	5.21×10^{-4}	5.21×10^{-4}

Table XIII: *Porous Object*, $\tau = 0.05$ - Reconstruction errors: total (ξ_{tot}), internal (ξ_{int}) and external (ξ_{ext}) errors.

	$SNR = 50dB$			
	$S=1$	$S=2$	$S=3$	$S=4$
$L^{(S)}$	6.00	1.50	1.50	1.50
$N^{(S)}$	100	208	208	208
$Q^{(S)}$	100	144	36	25
	$SNR = 20dB$			
	$S=1$	$S=2$	$S=3$	$S=4$
$L^{(S)}$	6.00	1.50	1.50	1.50
$N^{(S)}$	100	208	208	208
$Q^{(S)}$	100	144	25	25
	$SNR = 10dB$			
	$S=1$	$S=2$	$S=3$	$S=4$
$L^{(S)}$	6.00	1.50	1.50	1.50
$N^{(S)}$	100	208	208	208
$Q^{(S)}$	100	144	36	25
	$SNR = 5dB$			
	$S=1$	$S=2$	$S=3$	$S=4$
$L^{(S)}$	6.00	1.80	1.80	1.80
$N^{(S)}$	100	208	208	208
$Q^{(S)}$	100	144	36	36

Table XIV: *Porous Object*, $\tau = 0.05$ - Investigation domain parameters: restricted investigation domain size $L^{(S)}$, total number of cells $N^{(S)}$ and number of cells within the restricted domain size $Q^{(S)}$.

1.2.3 Porous Object, $\ell = 1.5\lambda$, $\tau = 0.15$ - IMSA-BCS reconstructed profiles

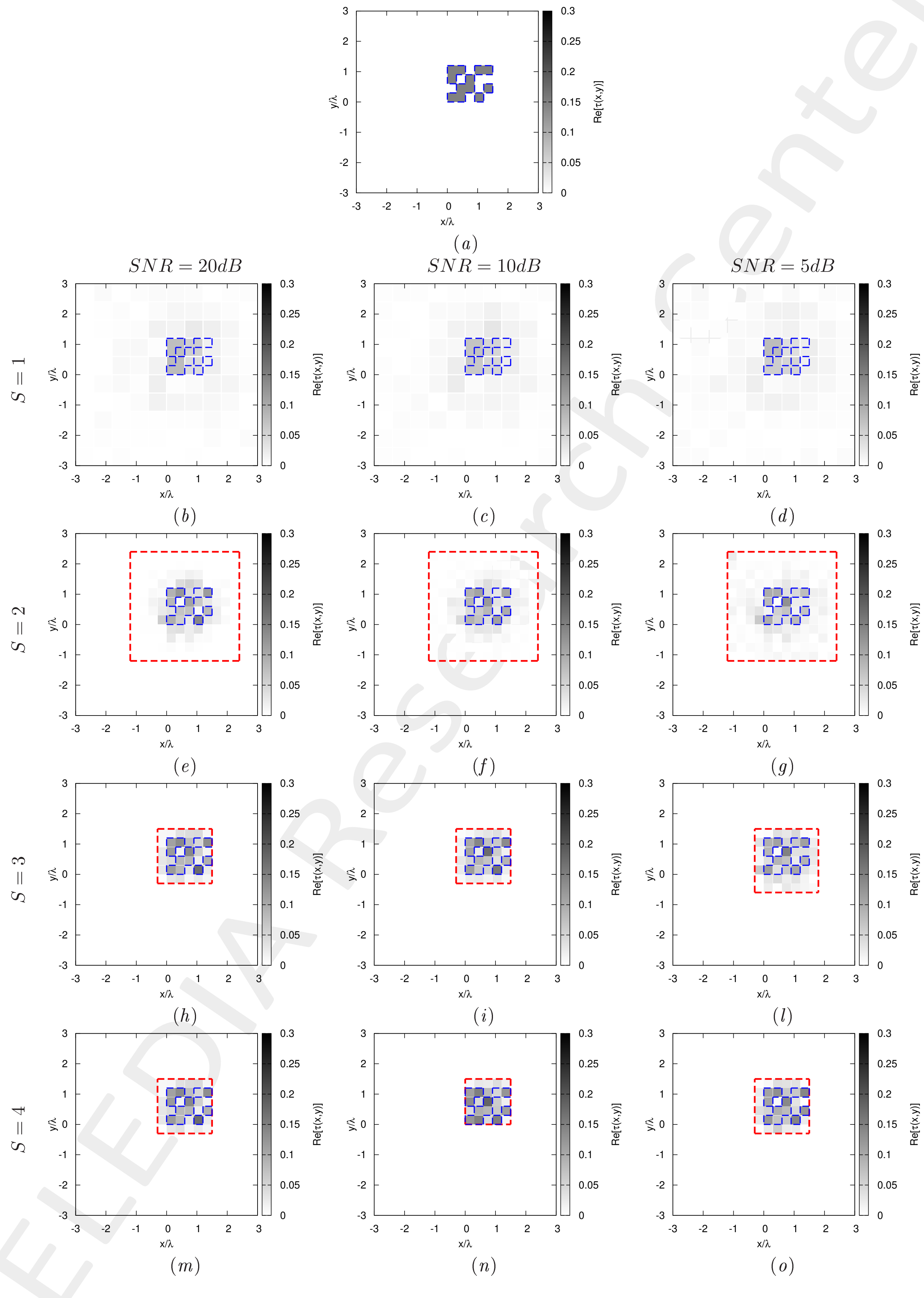

Figure 13: *Porous Object*, $\tau = 0.10$ - (a) Actual profile and (b)-(o) IMSA-BCS reconstructed profiles for $(b)(e)(h)$ $SNR = 20$ [dB], $(c)(f)(i)$ $SNR = 10$ [dB] and $(d)(g)(l)$ $SNR = 5$ [dB] at the step (b)-(d) $S = 1$, (e)-(g) $S = 2$, and (h)-(l) $S = 3$.

	$SNR = 50dB$			
	$S = 1$	$S = 2$	$S = 3$	$S = 4$
ξ_{tot}	8.27×10^{-3}	4.09×10^{-3}	3.13×10^{-3}	3.13×10^{-3}
ξ_{int}	8.08×10^{-2}	5.31×10^{-2}	4.29×10^{-2}	4.29×10^{-2}
ξ_{ext}	5.61×10^{-3}	2.29×10^{-3}	1.69×10^{-3}	1.69×10^{-3}
	$SNR = 20dB$			
	$S = 1$	$S = 2$	$S = 3$	$S = 4$
ξ_{tot}	8.41×10^{-3}	4.13×10^{-3}	2.98×10^{-3}	2.98×10^{-3}
ξ_{int}	7.98×10^{-2}	5.26×10^{-2}	3.83×10^{-2}	3.83×10^{-2}
ξ_{ext}	5.62×10^{-3}	2.35×10^{-3}	1.65×10^{-3}	1.65×10^{-3}
	$SNR = 10dB$			
	$S = 1$	$S = 2$	$S = 3$	$S = 4$
ξ_{tot}	8.91×10^{-3}	4.32×10^{-3}	3.06×10^{-3}	2.43×10^{-3}
ξ_{int}	8.35×10^{-2}	5.38×10^{-2}	4.04×10^{-2}	2.90×10^{-2}
ξ_{ext}	6.02×10^{-3}	2.40×10^{-3}	1.67×10^{-3}	1.25×10^{-3}
	$SNR = 5dB$			
	$S = 1$	$S = 2$	$S = 3$	$S = 4$
ξ_{tot}	9.61×10^{-3}	5.32×10^{-3}	4.01×10^{-3}	3.14×10^{-3}
ξ_{int}	8.48×10^{-2}	6.20×10^{-2}	4.96×10^{-2}	3.43×10^{-2}
ξ_{ext}	6.40×10^{-3}	2.94×10^{-3}	2.20×10^{-3}	1.70×10^{-3}

Table XV: *Porous Object*, $\tau = 0.15$ - Reconstruction errors: total (ξ_{tot}), internal (ξ_{int}) and external (ξ_{ext}) errors.

	$SNR = 50dB$			
	$S = 1$	$S = 2$	$S = 3$	$S = 4$
$L^{(S)}$	6.00	1.80	1.80	1.80
$N^{(S)}$	100	208	208	208
$Q^{(S)}$	100	144	36	36
	$SNR = 20dB$			
	$S = 1$	$S = 2$	$S = 3$	$S = 4$
$L^{(S)}$	6.00	1.80	1.80	1.80
$N^{(S)}$	100	208	208	208
$Q^{(S)}$	100	144	36	36
	$SNR = 10dB$			
	$S = 1$	$S = 2$	$S = 3$	$S = 4$
$L^{(S)}$	6.00	1.50	1.50	1.50
$N^{(S)}$	100	208	208	208
$Q^{(S)}$	100	144	36	25
	$SNR = 5dB$			
	$S = 1$	$S = 2$	$S = 3$	$S = 4$
$L^{(S)}$	6.00	1.80	1.80	1.80
$N^{(S)}$	100	208	208	208
$Q^{(S)}$	100	144	49	36

Table XVI: *Porous Object*, $\tau = 0.05$ - Investigation domain parameters: restricted investigation domain size $L^{(S)}$, total number of cells $N^{(S)}$ and number of cells within the restricted domain size $Q^{(S)}$.

1.2.4 Porous Object, $\ell = 1.5\lambda$, $\tau = 0.20$ - IMSA-BCS reconstructed profiles

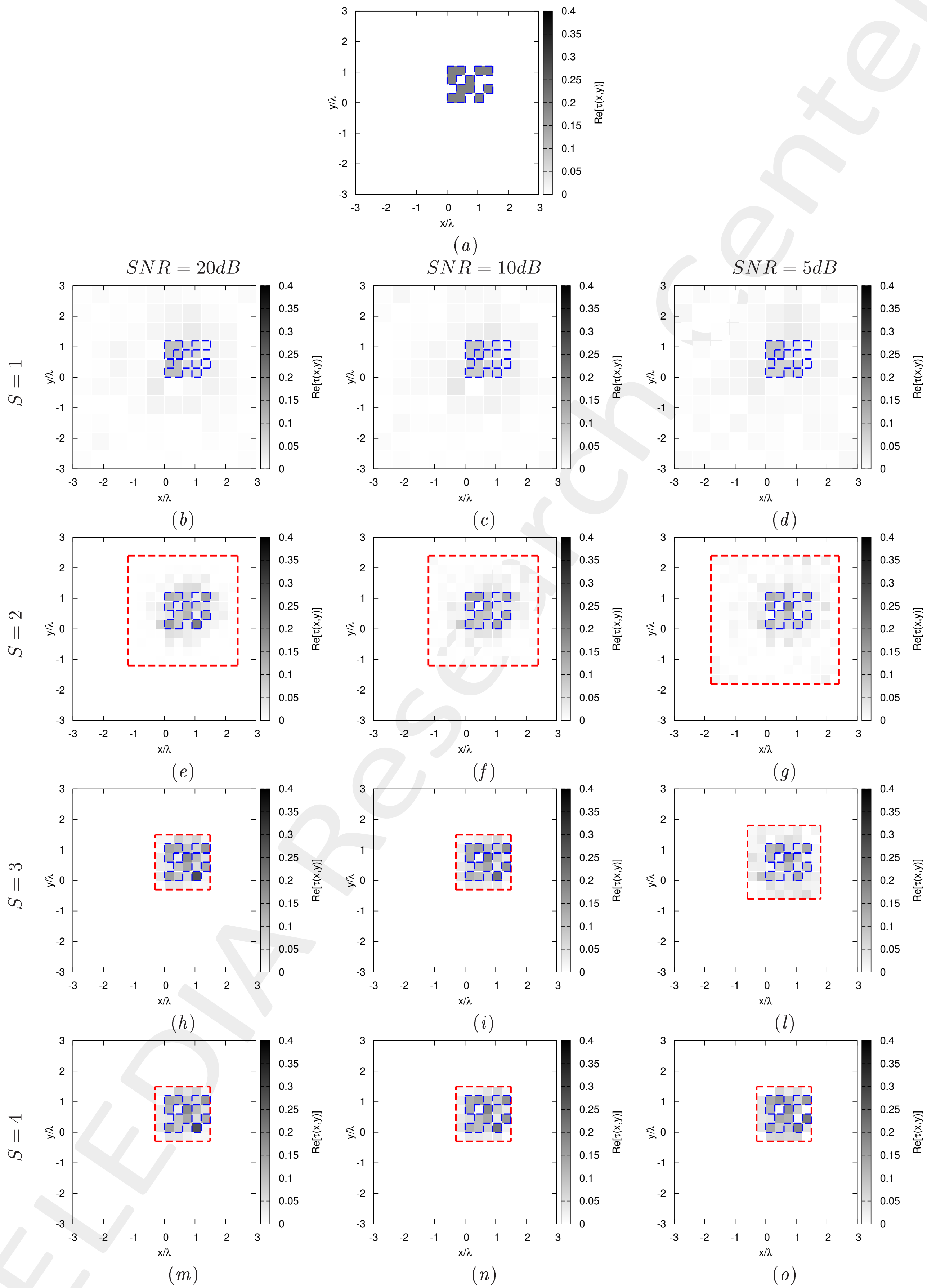

Figure 14: *Porous Object*, $\tau = 0.20$ - (a) Actual profile and (b)-(o) IMSA-BCS reconstructed profiles for $(b)(e)(h)$ $SNR = 20$ [dB], $(c)(f)(i)$ $SNR = 10$ [dB] and $(d)(g)(l)$ $SNR = 5$ [dB] at the step (b)-(d) $S = 1$, (e)-(g) $S = 2$, and (h)-(l) $S = 3$.

	$SNR = 50dB$			
	$S=1$	$S=2$	$S=3$	$S=4$
ξ_{tot}	1.10×10^{-2}	6.19×10^{-3}	4.63×10^{-3}	4.63×10^{-3}
ξ_{int}	1.02×10^{-1}	7.96×10^{-2}	6.28×10^{-2}	6.28×10^{-2}
ξ_{ext}	7.43×10^{-3}	3.44×10^{-3}	2.39×10^{-3}	2.39×10^{-3}
	$SNR = 20dB$			
	$S=1$	$S=2$	$S=3$	$S=4$
ξ_{tot}	1.11×10^{-2}	5.86×10^{-3}	4.51×10^{-3}	4.51×10^{-3}
ξ_{int}	1.05×10^{-1}	7.45×10^{-2}	6.11×10^{-2}	6.11×10^{-2}
ξ_{ext}	7.50×10^{-3}	3.26×10^{-3}	2.29×10^{-3}	2.29×10^{-3}
	$SNR = 10dB$			
	$S=1$	$S=2$	$S=3$	$S=4$
ξ_{tot}	1.20×10^{-2}	6.26×10^{-3}	4.23×10^{-3}	4.23×10^{-3}
ξ_{int}	1.09×10^{-1}	7.70×10^{-2}	5.01×10^{-2}	5.01×10^{-2}
ξ_{ext}	7.99×10^{-3}	3.52×10^{-3}	2.22×10^{-3}	2.22×10^{-3}
	$SNR = 5dB$			
	$S=1$	$S=2$	$S=3$	$S=4$
ξ_{tot}	1.39×10^{-2}	8.49×10^{-3}	6.74×10^{-3}	5.19×10^{-3}
ξ_{int}	1.12×10^{-1}	8.62×10^{-2}	8.10×10^{-2}	5.12×10^{-2}
ξ_{ext}	9.12×10^{-3}	4.78×10^{-3}	3.57×10^{-3}	2.66×10^{-3}

Table XVII: *Porous Object*, $\tau = 0.20$ - Reconstruction errors: total (ξ_{tot}), internal (ξ_{int}) and external (ξ_{ext}) errors.

	$SNR = 50dB$			
	$S=1$	$S=2$	$S=3$	$S=4$
$L^{(S)}$	6.00	1.80	1.80	1.80
$N^{(S)}$	100	208	208	208
$Q^{(S)}$	100	144	36	36
	$SNR = 20dB$			
	$S=1$	$S=2$	$S=3$	$S=4$
$L^{(S)}$	6.00	1.80	1.80	1.80
$N^{(S)}$	100	208	208	208
$Q^{(S)}$	100	144	36	36
	$SNR = 10dB$			
	$S=1$	$S=2$	$S=3$	$S=4$
$L^{(S)}$	6.00	1.80	1.80	1.80
$N^{(S)}$	100	208	208	208
$Q^{(S)}$	100	144	36	36
	$SNR = 5dB$			
	$S=1$	$S=2$	$S=3$	$S=4$
$L^{(S)}$	6.00	1.80	1.80	1.80
$N^{(S)}$	100	247	247	247
$Q^{(S)}$	100	196	64	36

Table XVIII: *Porous Object*, $\tau = 0.05$ - Investigation domain parameters: restricted investigation domain size $L^{(S)}$, total number of cells $N^{(S)}$ and number of cells within the restricted domain size $Q^{(S)}$.

1.2.5 Porous Object, $\ell = 1.5\lambda$, $\tau = 0.20$ - IMSA-BCS multi-resolution grids

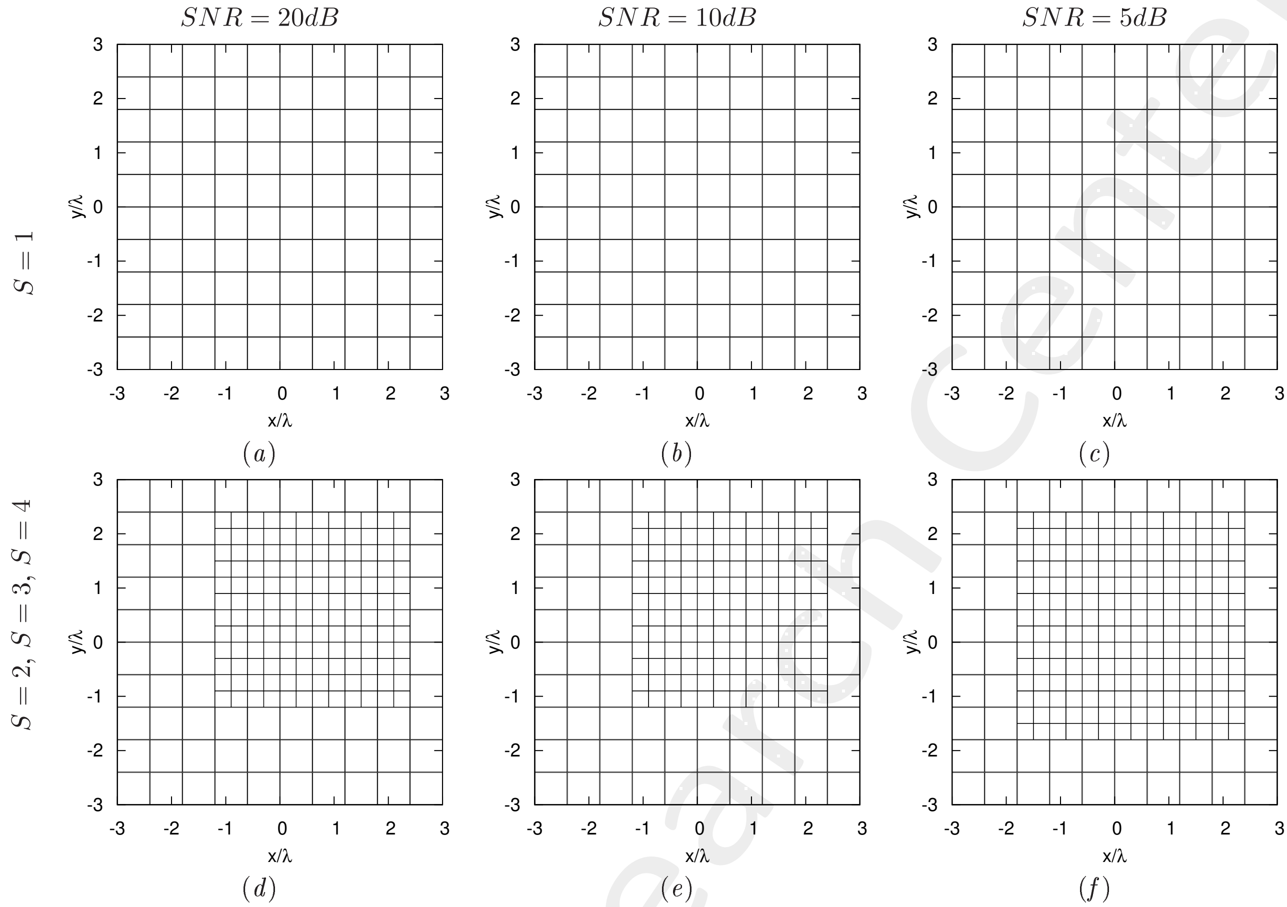

Figure 15: *Porous Object*, $\tau = 0.20$ - Example of IMSA-BCS multi-resolution grids for $(a)(d)$ $SNR = 20$ [dB], $(b)(e)$ $SNR = 10$ [dB] and $(c)(f)$ $SNR = 5$ [dB] at the step (a)-(c) $S = 1$ and (d)-(f) $S = 2$, 3 4.

1.2.6 Porous Object, $\ell = 1.5\lambda$ - Resume: Errors vs. *IMSA* step, S

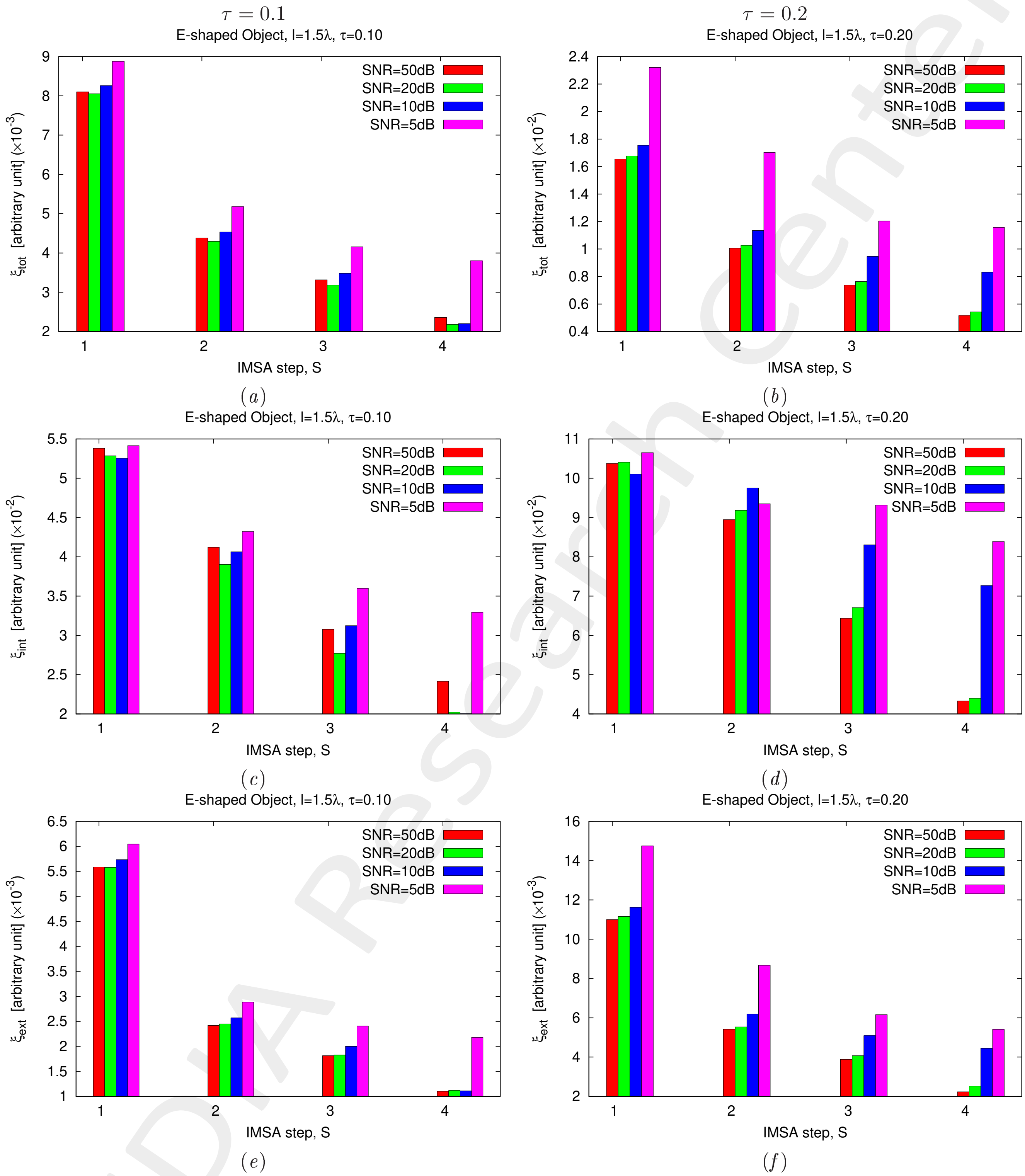

Figure 16: *Porous Object* - Reconstruction errors vs. *IMSA* step, S: $(a)(b)$ total error, $(c)(d)$ internal error and $(e)(f)$ external error for $(a)(c)(e)$ $\tau = 0.1$ and $(b)(d)(f)$ $\tau = 0.2$.

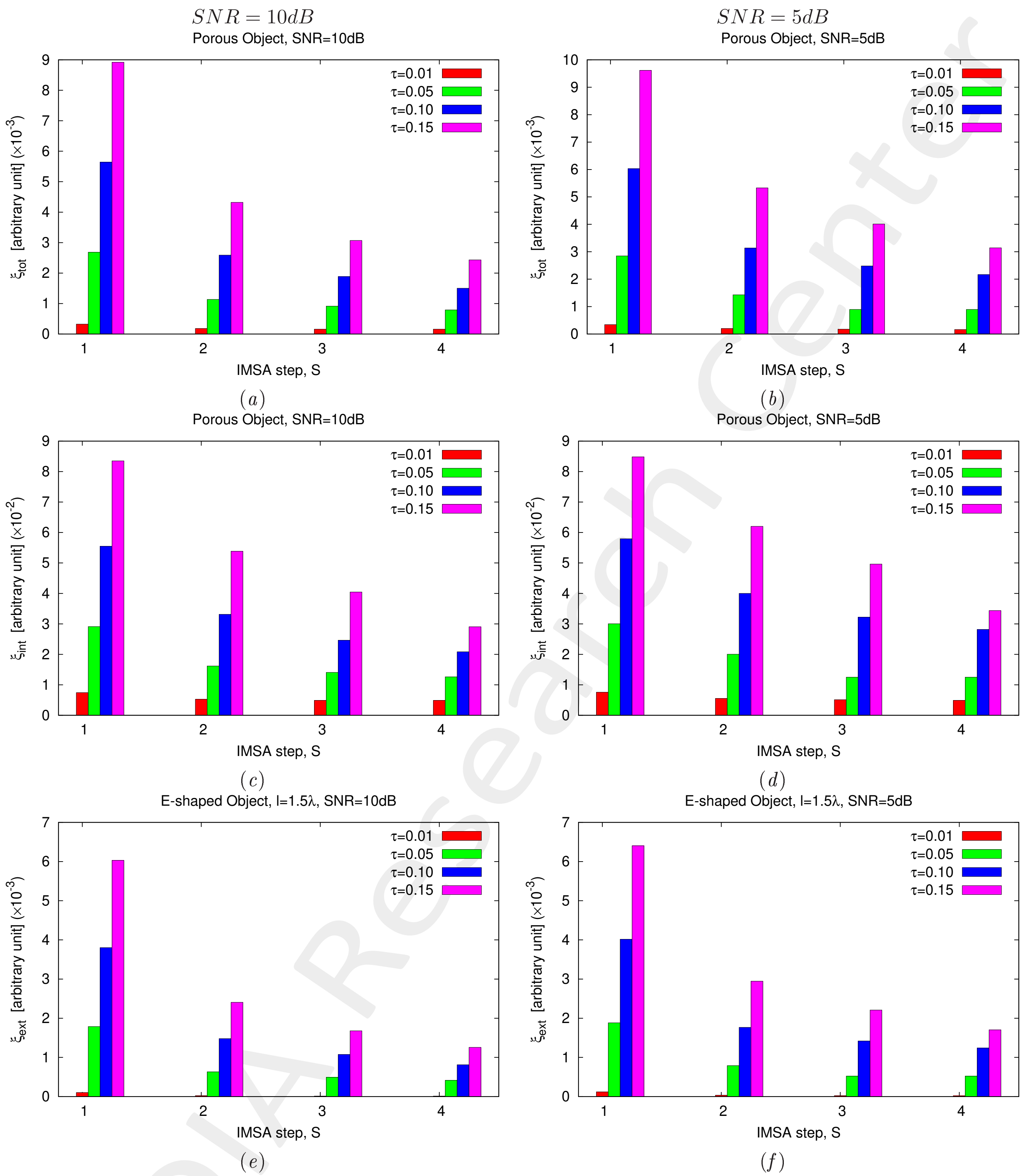

Figure 17: *Porous Object* - Reconstruction errors vs. $IMSA$ step, S: $(a)(b)$ total error, $(c)(d)$ internal error and $(e)(f)$ external error for $(a)(c)(e)$ $SNR = 10dB$ and $(b)(d)(f)$ $SNR = 5dB$.

More information on the topics of this document can be found in the following list of references.

References

[1] M. Salucci, G. Oliveri, and A. Massa, “GPR prospecting through an inverse scattering frequency-hopping multi-focusing approach,” *IEEE Trans. Geosci. Remote Sens.*, vol. 53, no. 12, pp. 6573-6592, Dec. 2015 (DOI: 10.1109/TGRS.2015.2444391).

[2] M. Salucci, L. Poli, N. Anselmi, and A. Massa, “Multifrequency Particle Swarm Optimization for enhanced multiresolution GPR microwave imaging,” *IEEE Trans. Geosci. Remote Sens.*, vol. 55, no. 3, pp. 1305-1317, Mar. 2017 (DOI: 10.1109/TGRS.2016.2622061).

[3] M. Salucci, L. Poli, and A. Massa, “Advanced multi-frequency GPR data processing for non-linear deterministic imaging,” *Signal Processing - Special Issue on ’Advanced Ground-Penetrating Radar Signal-Processing Techniques,’* vol. 132, pp. 306-318, Mar. 2017 (DOI: 10.1016/j.sigpro.2016.06.019).

[4] N. Anselmi, G. Oliveri, M. Salucci, and A. Massa, “Wavelet-based compressive imaging of sparse targets,” *IEEE Trans. Antennas Propag.*, vol. 63, no. 11, pp. 4889-4900, Nov. 2015 (DOI: 10.1109/TAP.2015.2444423).

[5] G. Oliveri, M. Salucci, N. Anselmi, and A. Massa, “Compressive sensing as applied to inverse problems for imaging: theory, applications, current trends, and open challenges,” *IEEE Antennas Propag. Mag. - Special Issue on "Electromagnetic Inverse Problems for Sensing and Imaging,"* vol. 59, no. 5, pp. 34-46, Oct. 2017 (DOI: 10.1109/MAP.2017.2731204).

[6] A. Massa, P. Rocca, and G. Oliveri, “Compressive sensing in electromagnetics - A review," *IEEE Antennas Propag. Mag.*, pp. 224-238, vol. 57, no. 1, Feb. 2015 (DOI: 10.1109/MAP.2015.2397092).

[7] N. Anselmi, L. Poli, G. Oliveri, and A. Massa, “Iterative multi-resolution bayesian CS for microwave imaging,” *IEEE Trans. Antennas Propag.*, vol. 66, no. 7, pp. 3665-3677, Jul. 2018 (DOI: 10.1109/TAP.2018.2826574).

[8] N. Anselmi, G. Oliveri, M. A. Hannan, M. Salucci, and A. Massa, “Color compressive sensing imaging of arbitrary-shaped scatterers,” *IEEE Trans. Microw. Theory Techn.*, vol. 65, no. 6, pp. 1986-1999, Jun. 2017 (DOI: 10.1109/TMTT.2016.2645570).

[9] G. Oliveri, N. Anselmi, and A. Massa, “Compressive sensing imaging of non-sparse 2D scatterers by a total-variation approach within the Born approximation,” *IEEE Trans. Antennas Propag.*, vol. 62, no. 10, pp. 5157-5170, Oct. 2014 (DOI: 10.1109/TAP.2014.2344673).

[10] L. Poli, G. Oliveri, and A. Massa, “Imaging sparse metallic cylinders through a local shape function Bayesian compressive sensing approach,” *J. Opt. Soc. Am. A*, vol. 30, no. 6, pp. 1261-1272, 2013 (DOI: 10.1364/JOSAA.30.001261).

[11] L. Poli, G. Oliveri, F. Viani, and A. Massa, “MT-BCS-based microwave imaging approach through minimum-norm current expansion," *IEEE Trans. Antennas Propag.*, vol. 61, no. 9, pp. 4722-4732, Sep. 2013 (DOI: 10.1109/TAP.2013.2265254).

[12] F. Viani, L. Poli, G. Oliveri, F. Robol, and A. Massa, “Sparse scatterers imaging through approximated multitask compressive sensing strategies," *Microwave Opt. Technol. Lett.*, vol. 55, no. 7, pp. 1553-1558, Jul. 2013 (10.1002/mop.27612).

[13] L. Poli, G. Oliveri, P. Rocca, and A. Massa, “Bayesian compressive sensing approaches for the reconstruction of two-dimensional sparse scatterers under TE illumination," *IEEE Trans. Geosci. Remote Sens.*, vol. 51, no. 5, pp. 2920-2936, May 2013 (DOI: 10.1109/TGRS.2012.2218613).

[14] L. Poli, G. Oliveri, and A. Massa, “Microwave imaging within the first-order Born approximation by means of the contrast-field Bayesian compressive sensing," *IEEE Trans. Antennas Propag.*, vol. 60, no. 6, pp. 2865-2879, Jun. 2012 (DOI: 10.1109/TAP.2012.2194676).

[15] G. Oliveri, L. Poli, P. Rocca, and A. Massa, “Bayesian compressive optical imaging within the Rytov approximation," *Optics Letters*, vol. 37, no. 10, pp. 1760-1762, 2012 (DOI: 10.1364/OL.37.001760).

[16] G. Oliveri, P. Rocca, and A. Massa, “A Bayesian compressive sampling-based inversion for imaging sparse scatterers," *IEEE Trans. Geosci. Remote Sens.*, vol. 49, no. 10, pp. 3993-4006, Oct. 2011 (DOI: 10.1109/TGRS.2011.2128329).

[17] G. Oliveri, M. Salucci, and N. Anselmi, “Tomographic imaging of sparse low-contrast targets in harsh environments through matrix completion," *IEEE Trans. Microw. Theory Tech.*, vol. 66, no. 6, pp. 2714-2730, Jun. 2018 (DOI: 10.1109/TMTT.2018.2825393).

[18] M. Salucci, A. Gelmini, L. Poli, G. Oliveri, and A. Massa, “Progressive compressive sensing for exploiting frequency-diversity in GPR imaging,” *J.Electromagn. Waves Appl.*, vol. 32, no. 9, pp. 1164-1193, 2018 (DOI: 10.1080/09205071.2018.1425160).